



## ORIGINAL ARTICLE

# Insight into the biosensing of graphene oxide: Present and future prospects



Deepali Sharma, Suvadhan Kanchi <sup>\*</sup>, Myalowenkosi I. Sabela, K. Bisetty <sup>\*</sup>

Department of Chemistry, Durban University of Technology, P.O. Box 1334, Durban 4000, South Africa

Received 1 June 2015; accepted 27 July 2015

Available online 8 August 2015

## KEYWORDS

Graphene oxide;  
Biosensor;  
Functionalization;  
Nanosheets;  
Nanoparticles

**Abstract** Graphene oxide, a century old material has attracted the interest of researchers owing to its specific 2D structure and unique electronic, optical, thermal, mechanical and electrochemical properties. The recent advancements in the field of biotechnology and biomedical engineering are targeted at exploring the biosensing applications of graphene oxide due to its biocompatibility. It is considered to be one of the most versatile materials, with wide range of applications which can be tailored by functionalization of the different oxygen containing groups present in the structure. In this review the focus is on the biosensing applications of graphene oxide, detection of analytes with high sensitivity and selectivity. This would give insight into the designing of feasible protocols for the analysis of therapeutic diseases and environmental safety, thereby improving the quality of human life.

© 2015 The Authors. Production and hosting by Elsevier B.V. on behalf of King Saud University. This is an open access article under the CC BY-NC-ND license (<http://creativecommons.org/licenses/by-nc-nd/4.0/>).

## 1. Introduction

The commercial success of any new material lies in its reproducibility and production at industrial scale with superior qualities. The present era is for the family of carbon based materials with graphene being a highly attractive and intensively investigated material due to its unique properties such

as enhanced electrical and thermal conductivity, high mechanical strength, optical transparency, good quantum hall effect and high impermeability to gases (Chua and Pumera, 2014). Graphene having  $sp^2$  carbons forms honeycomb lattice which has paved its way since its discovery creating an enormous interest in the scientific community.

Among various forms of graphene such as nanotubes, fullerenes, graphite oxide/graphene oxide/graphitic oxide (GO) also known as graphitic acid, a century old material has focused tremendous interest. It was first prepared by Benjamin C. Brodie who was chemist in Oxford in 1859. He treated graphite with a mixture of potassium chlorate and fuming nitric acid (Brodie, 1859) and termed it as 'graphitic acid' since it dispersed in basic solution but not in acidic media. In 1898, almost after 40 years of Brodie's discovery, the oxidation method was improvised by L. Staudenmaier by adding potassium chlorate in limited amounts along with concentrated sulfuric acid rather than adding in a single step.

<sup>\*</sup> Corresponding authors. Tel.: +27 31 3736008/2311; fax: +27 86 6740243.

E-mail addresses: [dpschem@gmail.com](mailto:dpschem@gmail.com) (D. Sharma), [ksuvadhan@gmail.com](mailto:ksuvadhan@gmail.com) (S. Kanchi), [myalosabela@gmail.com](mailto:myalosabela@gmail.com) (M.I. Sabela), [bisettyk@dut.ac.za](mailto:bisettyk@dut.ac.za) (K. Bisetty).

Peer review under responsibility of King Saud University.



Production and hosting by Elsevier

Though this change in the method resulted in the same C:O (2:1) ratio as in Brodie's case this reaction avoided multiple repetition of oxidation (Staudenmaier, 1898).

A very efficient, fast and safe route which involves the use of  $\text{H}_2\text{SO}_4$ ,  $\text{NaNO}_3$  and  $\text{KMnO}_4$  was developed by Hummers and Offemann in 1957 and is widely used till now with slight modifications. (Hummers and Offemann, 1958). To control the thickness of the GO layers by adjusting thickness, simpler and environment-friendly 'bottom-up' approach has been developed where glucose is the sole source. The method is known as Tang-Lau and has an advantage over other methods which involves the use of strong oxidizers (Tang et al., 2012). The carbohydrates containing C, H and O atoms in the ratio  $\sim 1:2:1$  act as a carbon source for the fabrication of graphene oxide nanosheets (GONs). The facile mechanism involves the dissolution of glucose in deionized (DI) water where polymerization occurs due to the dehydration of hydroxyl, carboxyl and carbonyl groups under hydrothermal conditions forming GONs. These sheets are transferred onto the surface of a substrate by dipping, lifting and finally rinsing with DI water to remove any residues. The final step involves the annealing of as-synthesized GON at a certain temperature to tune its electrical, optical and structural properties. The schematic mechanism has been shown in Fig. 1.

The most common naturally occurring source of graphite is 'flake graphite' and GO prepared from this is readily dispersed in water. A method has been hypothesized in the literature where 9:1 mixture of concentrated  $\text{H}_2\text{SO}_4/\text{H}_3\text{PO}_4$  was used to prepare improved GO with introduction of few defects thereby providing greater amount of hydrophilic oxidized

graphite material (Marcano et al., 2010). This method did not evolve toxic gases and produced high yield of material.

## 2. Structure and electrochemical aspects of graphene oxide (GO)

It is very important to fully understand the structure of GO which is composed of C, O and H atoms before it could be used for fundamental applications especially taking into consideration some of the biosensing properties. Since, GO is a derivative of graphene it retains the layer structure and contains  $\text{sp}^3$  hybridized carbon atom. Depending on the synthesis process, and different types of oxygen species in groups such as carbonyl, carboxyl, epoxy, hydroxy and oxidation, GO exhibits variable structures and properties (Inagaki and Kang, 2014). The different functional groups put a profound impact on the properties of the material which could lead to the potential applications in different fields of science and engineering (Compton and Nguyen, 2010). Till date, different models of GO have been proposed (Fig. 2). The first structural model for GO was proposed by Hofmann and Holst in 1939 with only epoxide groups. It was supposed that the oxygen atom was bound to carbon atoms of hexagon layer by epoxide linkages with ideal formula  $\text{C}_2\text{O}$ . In 1947, Ruess suggested a model taking into consideration the hydrogen atoms of GO and indicated the  $\text{sp}^3$  hybridization form of basal plane structure. This model was revised by Scholz-Boehm consisting of ribbons of conjugated carbon atom eliminating the epoxide groups. Lerf and co-workers, suggested a structural model on the basis of  $^1\text{H}$  NMR and solid state NMR spectra with randomly distributed aromatic and wrinkled regions. From the XRD

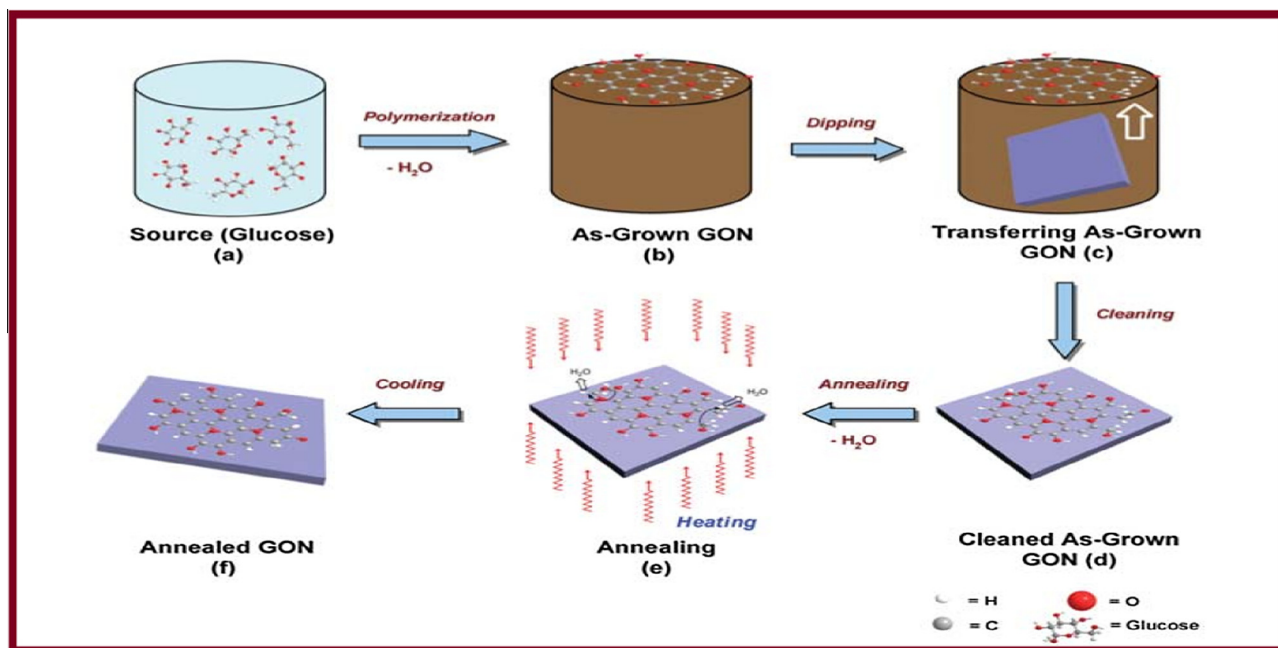


**Figure 1** Schematic illustration of preparing a GON. (a) Glucose dissolved in DI water to obtain a colorless transparent source solution. (b) Under hydrothermal conditions, polymerization occurs as glucose molecules dehydrate intermolecularly to form a GON which floats onto the surface of the solution due to its hydrophobic property. (c) The as-grown GON can be transferred onto any substrate by dipping and lifting. (d) The transferred GON is rinsed by dipping into DI water to remove the residue. (e) The as-grown GON is annealed at a certain temperature to dehydrate and graphitize for tuning its electrical, optical and structural properties. (f) The annealed GON with desired thickness and electrical properties. Reproduced with permission Tang et al. (2012).

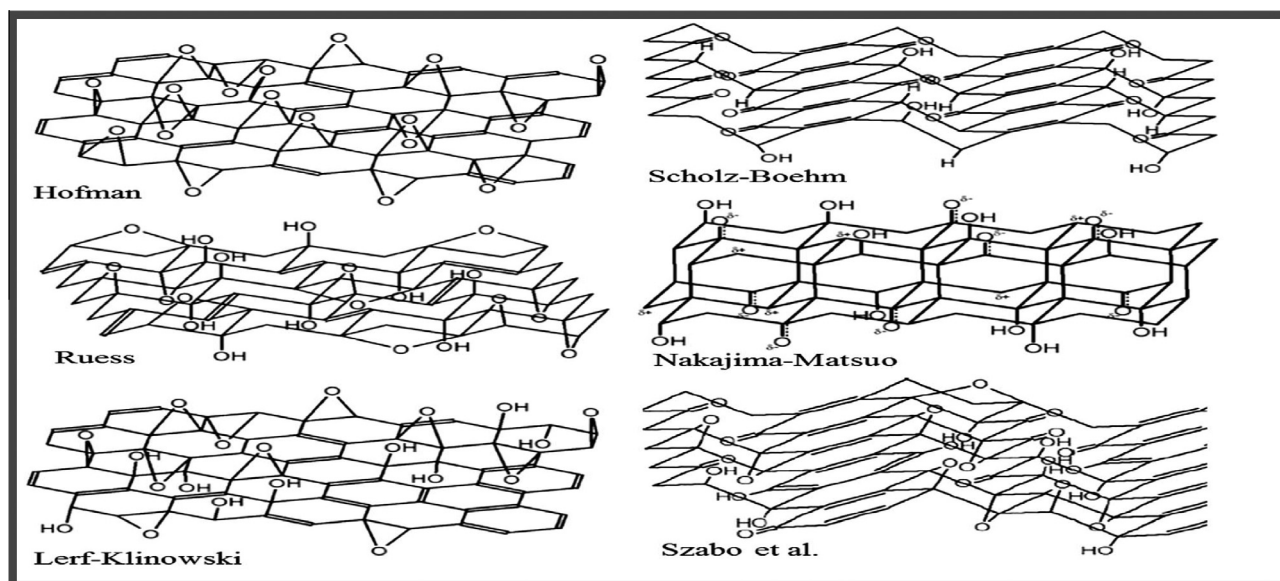


**Figure 2** Proposed structures of graphite oxides. Reproduced with permission Inagaki and Kang (2014).

information, Nakajima et al., suggested a poly-like model  $(C_2F)_n$  by fluorination of GO. Szabo et al.'s model is a combination of Ruess and Scholz-Boehm skeleton model. In this there was a ribbon-like arrangement of flat carbon hexagons connected by C=C double bonds (Zhao et al., 2015a, 2015b).

It has been reported that the layers in the GO are buckled and the spacing between the layers is almost twice that in the parent graphene. The interplanar spacing increases (up to 1.2 nm in saturated state) on immersing the GO in water. The water layer is inserted in between the GO layers. Thus, GO is hydrophilic and gets hydrated as soon as immersed in water. Apart from water, other polar solvents such as alcohols are also incorporated in the layers but to different extent. Separation of GO layers is proportional to the size of alcohol molecule (Krishnan et al., 2012; Talyzin et al., 2008, 2009; Dreyer et al., 2014; Eigler et al., 2013; Singh et al., 2011).

In terms of electrical conductivity, GO is termed as an insulator due to the disruption of its  $sp^2$  bonding networks. The reduction of GO leads to the recovery of its honeycomb hexagonal lattice and its electrical conductivity. The functionalization of GO changes its properties thereby making it more adaptable for lot of applications. In GO, carbonyl and carboxyl groups are present along the edges which leads to the defects in the sheet whereas hydroxyl and epoxide groups are present on the basal plane (Lerf et al., 1998). The presence of oxygen containing groups renders hydrophilicity to GO and also makes it thermally unstable. These groups present reactive sites used for chemical modification by using selective organic moieties thus, making GO organophilic. Though chemically modified GO is less conductive in nature as compared to pristine graphene reduction is overcome by the enhancement of conductive properties resulting from the dispersion of graphene layers into the matrix or solvent. Ionic liquids (ILs) have been used to functionalize and exfoliate GO. The electron negative  $\pi$ -bonds and deprotonation of functional groups of GO attract cations present in ILs by Brownian motion rendering them to be strongly adsorbed on the graphene sheet surface. As a result, a charged diffuse layer

is formed which causes repulsion between charged graphene sheets. These sheets can be easily separated by ultrasonication to promote cation mobility. After the functionalization or reduction, ILs due to their high dielectric constant, provide shielding for  $\pi$ - $\pi$  restacking and van der Waals interactions. Thus, ILs act as stabilizers by preventing agglomeration of graphene sheets in GO during functionalization thereby retaining the prominent inherent properties of the sheets. In contrast to other surfactants and stabilizers, ILs can be easily removed as they are water soluble (Fu et al., 2013). The complete mechanism has been pictorially depicted in Fig. 3.

GO has become a material of great attention for experimentalists and theoreticians in recent years due to its unique properties such as high surface area, low cost of manufacture, good colloid condition, optical and electronic properties (Morales-Narváez and Merkoçi, 2012; Park and Ruoff, 2009; Loh et al., 2010; Zhu et al., 2010; Novoselov, 2011; Zubir et al., 2014; He and Gao, 2010). It is widely applicable in the fields of biotechnology, bioengineering, drug delivery, imaging of cells and biosensors as it is biocompatible. The biocompatibility of GO has been studied in the literature where bacterial cellulose/graphene oxide (BC/GO) composites have been reported to exhibit good antibacterial activity against *Escherichia coli* (95.61%) and *Staphylococcus aureus* (65.35%). The incorporation of GO nanosheets within BC improves the antibacterial activity due to the formation of a strong hydrogen bond between carboxyl group of GO and hydroxyl group of BC. The biocompatibility of GO was assessed by the inclusion of 8 wt% of it in BC where no cell cytotoxicity was observed (Shao et al., 2015). The in vivo biocompatibility study of nGO-PEG, RGO-PEG and nRGO-PEG revealed that after administering them through oral route, these were found to be present in high quantities in stomach and intestine and not in other major organs. The low levels were detected after one day and no trace was detected after one week. Thus, these were found to be poorly adsorbed in gastrointestinal tract due to their rapid excretion (Yang et al., 2013a, 2013b). Due to widespread demand, the

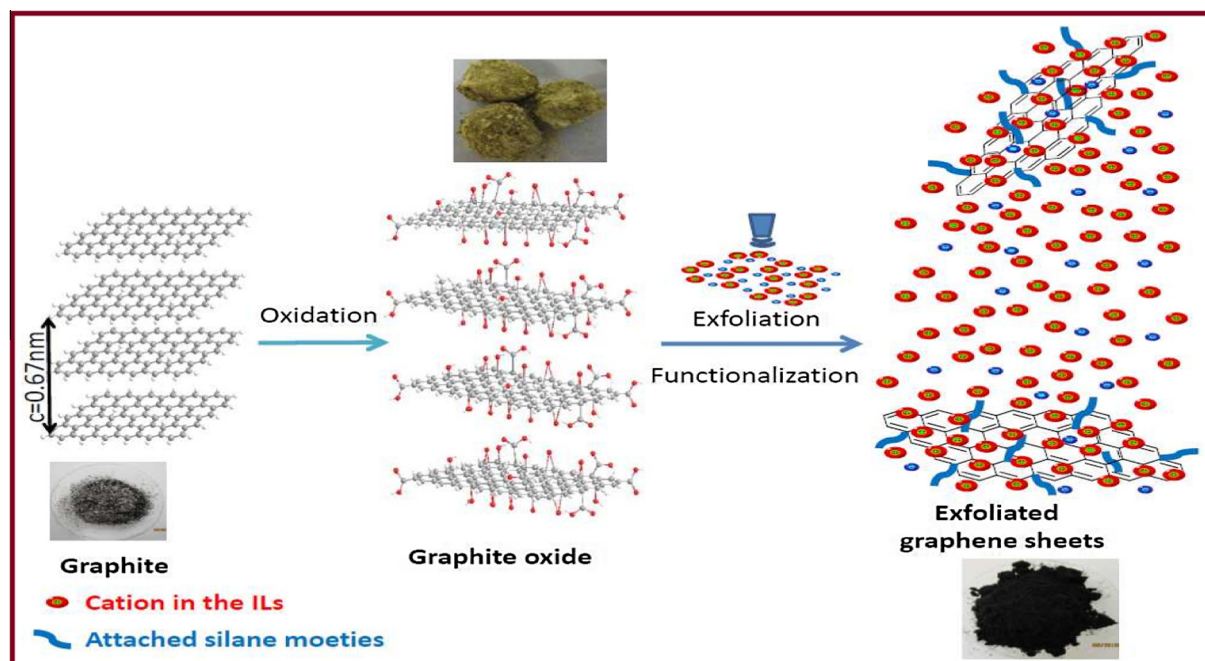


**Figure 3** Proposed mechanism of simultaneous exfoliation and functionalization/reduction of graphite oxide with the aid of the IL. Reproduced with permission Fu et al. (2013).

production of GO at industrial level has also emerged. This review is focused on the biosensor properties of GO and would highlight some of the upcoming applications for biosensing molecules.

Different approaches have been developed for the synthesis of graphene, such as mechanical cleavage (Novoselov et al., 2004, 2005), epitaxial growth (Forbeaux et al., 1998; Cambaz et al., 2008), chemical vapor deposition (Kim et al., 2009; Li et al., 2009), electrochemical exfoliation of graphite (Wang et al., 2011a, 2011b; Lu et al., 2009a, 2009b, 2009c; Qi et al., 2011; Liu et al., 2008) and reduction of GO that is derived from chemical exfoliation of graphite (Compton et al., 2011). Recently non-covalent exfoliation of graphite by sonication in liquid phase has also been reported (Hernandez et al., 2008; Xia et al., 2013). Of all these approaches, the reduction of GO is regarded as one of the most promising routes for the mass production of graphene at a low cost and with high yield, although only partially restore the properties of pristine graphene. There are a number of routes for the reduction of GO such as chemical reduction (Wang et al., 2008a, 2008b; Stankovich et al., 2006a, 2006b), thermal reduction (Liu et al., 2013a, 2013b; Gao et al., 2010), photocatalytic reduction (Williams et al., 2008; Akhavan, 2011) and electrochemical reduction. Typically, the chemical reduction of GO route involves the use of reducing agents such as hydrazine (Peng et al., 2011; Zhu et al., 2009), dimethylhydrazine (Stankovich et al., 2006a, 2006b), metal hydrazides (Shin et al., 2009; Chua and Pumera, 2013) and hydroquinone (Wang et al., 2008a, 2008b). The excessive use of reducing agents could contaminate the resulting product (Guo et al., 2009) and is even harmful to human health and the environment (Paredes et al., 2011).

Moreover, some of oxygen functionalities in GO are selective and could not be removed completely with only one reductant treatment (Pariasamy and Thirumalaikumar, 2000; Wang

et al., 2009a, 2009b). On the other hand, the thermal reduction route involves the use of high temperature to remove the oxygen functionalities, which would result in high production cost in addition to tedious control of experimental conditions. The electrochemical reduction of GO is directly carried out using an aqueous colloidal suspension in the presence of phosphate buffer solution. However, other electrolytes, such as NaCl and Na<sub>2</sub>SO<sub>4</sub> (Hilder et al., 2011) have been reported as supporting electrolyte in GO colloidal suspension. The electrochemical reduction process can be performed with cyclic voltammetry (Liu et al., 2011a, 2011b, 2011c; Jiang et al., 2012), linear sweep voltammetry mode at a constant potential mode (Chang et al., 2012; Ping et al., 2011) in a standard three electrode system at ambient temperature. The electrochemical reduction takes place when GO sheets placed adjacent to the electrode accept electrons thereby yielding insoluble electrochemically reduced GO that is attached directly onto the electrode surface (Chen et al., 2011). The concentration of the electrolyte is often correlated to the overall conductivity of the medium. Hilder et al., reported that the conductivity of the medium is a critical parameter for the formation of high quality films during the electrochemical reduction of GO from an aqueous suspension. The optimal conductivity range was found to be between 4 and 25 mS cm<sup>-1</sup> for neutral pH media (0.5 mg mL<sup>-1</sup> GO and 0.25 M NaCl) at a reduction potential of -1.2 V with respect to saturated calomel electrode (SCE). In addition to the conductivity of the medium, the selection of the appropriate pH (1.5–12.5) for the medium is also essential to ensure good deposition of the electrochemically reduced GO onto the electrode surface (Hilder et al., 2011). The electrochemical reduction of GO is commonly attained by applying a constant potential reduction or cyclic voltammetric technique. However, other electrochemical techniques such as linear sweep voltammetry (Ping et al., 2011) and differential pulse voltammetry (Guo et al., 2009) have also been reported.

By the constant potential technique, a constant negative potential is applied over a period of time to fully reduce all of the GO sheets in the suspension. As the GO is consumed, the current decreases, approaching zero when the conversion is complete. The selection of the appropriate cathodic reduction potential and time is crucial for the complete reduction of GO. It is found that more negative potential increases the GO reduction rate. Guo et al., showed that the C=O functional groups in GO could be converted at  $-1.3$  V (vs. SCE). Although the oxygen content in the electrochemical reduced GO decreases with the use of more negative potential, several studies (Guo et al., 2009; Hilder et al., 2011) have reported that applying a potential more negative than  $-1.5$  V (vs. SCE) could lead to hydrogen gas bubble evolution from the reduction of water, in turn creating a physical barrier that hinders the GO sheets from approaching the working electrode and completing the electrode chemical reduction process. The main advantage of cyclic voltammetry as compared to the constant potential reduction is that it provides information about redox potential (Liu et al., 2011a, 2011b, 2011c) and the reversibility (Jiang et al., 2012) of the reaction. Typically, the electrochemical reduction of GO from aqueous suspension is carried out in the potential range of  $0$ – $1.5$  V. Scan rates in the range of  $20$ – $100$   $\text{mV s}^{-1}$  have been reported (Chen et al., 2011; Liu et al., 2011a, 2011b, 2011c; Dogan et al., 2013). It has been noted that the cyclic voltammogram obtained from an aqueous suspension at a working electrode exhibits two cathodic current peaks (Chen et al., 2011; Liu et al., 2011a, 2011b, 2011c; Dogan et al., 2013). Dogan et al., reported that the two peaks were in the range of  $-0.4$  to  $-0.6$  V (peak-I) and  $-0.6$  V to  $-1.0$  V (peak-II) with respect to the Ag/AgCl, 3 M NaCl electrode. Some researchers (Chen et al., 2011; Liu et al., 2011a, 2011b, 2011c; Dogan et al., 2013) attributed the cathodic peak-II to the irreversible electrochemical reduction process of GO. The peak-I was ascribed to oxygen containing groups on the graphene plane that were too stable to be reduced using the cyclic voltammetric technique.

### 3. Scope of the review

This review article discusses the recent advancements in the utilization of GO based biosensors. The efficiency of GO based biosensors depends on their functionalization under appropriate conditions without the minimum loss of their inherent properties. Extensive research has been carried out on nano-material based electrochemical biosensors; however they suffer from limitations of sensitivity, cost of production, detection time and stability. The present review is mainly targeted at the biosensing properties of GO based biosensors coupled with NPs and also focuses on the recent applications of these biosensors in the sensitive detection of Herpes simplex virus (HSV-1) which infected more than half of the world population. Although there are many challenges which are to be overcome the initial thrust in this research would unravel the potentials of GO in the biomedical field.

### 4. Biosensing of graphene oxide (GO)

From the prospective of improving the quality of human life, detection of wide range of molecules with high selectivity and sensitivity, therapeutic analysis of diseases, and

environment safety, biosensing is very important. GO and reduced rGO are used for different bioapplications due to their unique ability to disperse in aqueous medium and large surface area. They have become promising materials in the designing of protocols for the early stage detection and treatment of diseases and also have risen as an effective biosensor for the sensing of different analytes (Nurunnabi et al., 2015). The defects present in the structure of GO are a boon for it rather being disadvantageous as electron transfer occurs at the edges and defects. The presence of oxygen containing functional groups renders the functionalization assisting in the biorecognition during biosensing (Pumera, 2011). According to the application and sensing mechanism, the functionalization of GO can be readily carried out.

A biosensor consists of two parts, receptor and a transducer. A receptor is a molecule which interacts with an analyte and transducer is a sensing platform which converts the chemical information into a signal (Fig. 4).

### 5. Sensing applications of graphene oxide

The properties of GO have been exploited for the sensing of wide range of inorganic and organic molecules. Fig. 5 depicts some of the biosensing application of GO which has been critically discussed in the present review. The feasible protocols for biosensing applications have been successfully formulated and applied in the different fields of science and engineering.

#### 5.1. Graphene oxide in the detection of DNA

Carbon nanotubes, nanodots and nanofibers have been used for the fast, selective, sensitive and cost-effective detection of biomolecules. Nowadays, GO has become an attractive and one of important materials from carbon family due to its unique characteristics which are being extensively explored.

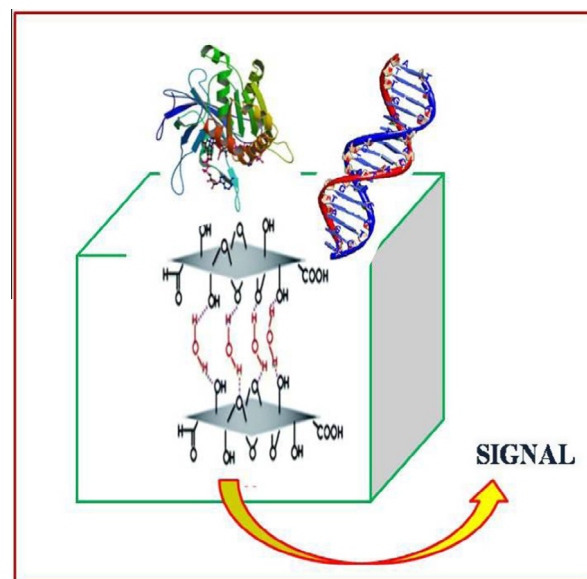


**Figure 4** Schematic illustration of biosensor with biomolecules (DNA or proteins) that act as receptor layer and GO as a transducer.

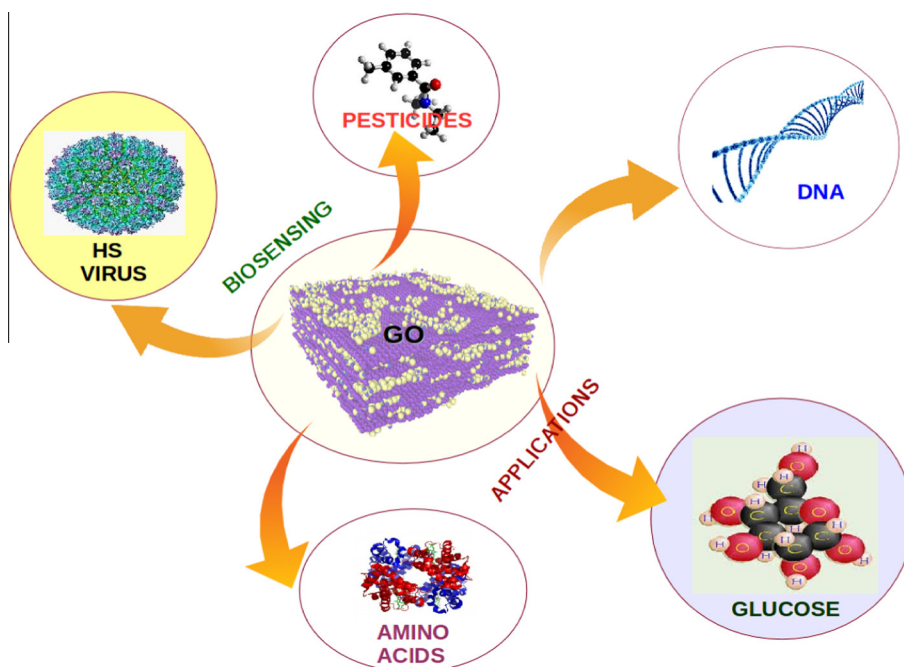


**Figure 5** Sensing applications of graphene oxide.

The presence of functional groups in GO renders strong hydrophilicity and good dispersibility in many solvents which plays a major role in processing and derivatization (Dikin et al., 2007; Sharma et al., 2013; Wang et al., 2009a, 2009b). The selective, sensitive, fast and cost-effective detection of biomolecules is very important in treatment and clinical diagnosis. In this regard, the fluorescence quenching ability of GO has been employed for the detection of multiple ssDNA (Lu et al., 2009a, 2009b, 2009c). GO binds to the dye-labeled ssDNA via non-covalent binding and quenches the fluorescence of the dye (step a, Fig. 6). The conformation of DNA is altered in the presence of a target molecule thereby disturbing the GO–ssDNA interaction. As a result, dye-labeled DNA is released from the surface of GO and fluorescence of dye is restored (step b, Fig. 6). This design based on enhanced fluorescence could be applied for the selective detection of the target molecule.

From theoretical calculations, it has been predicted that graphene is a super quencher with long-range nanoscale energy

transfer (Swathi and Sebastian, 2008, 2009) and forms a basis for a convenient strategy that can analyze multicolor DNA. The 'mix-and-detect' strategy is a modified of what was proposed by Lu et al. (2009a, 2009b, 2009c), being more sensitive and rapid. It was found that fluorophores such as FAM (carboxyfluorescein) and ROX (6-carboxy-X-rhodamine) were nonfluorescent in the presence of GO due to their strong adsorption on its surface and long-range energy transfer from dye to GO (He et al., 2010). Though both DNA and GO are negatively charged the fluorescence of FAM-tagged ssDNA was rapidly quenched by GO. The advantage of this biosensor involves the facile synthesis of GO in bulk with large planar surface able to analyze multiple molecular targets in the same solution, rapid, sensitive and low cost.

Regarding the adsorption of ssDNA on GO surface, it is very critical to understand whether the adsorption of DNA takes place directly on the surface of GO or in the solution phase which is important to improve the existing design of biosensors. In the literature,  $\pi$ - $\pi$  stacking, hydrophobic

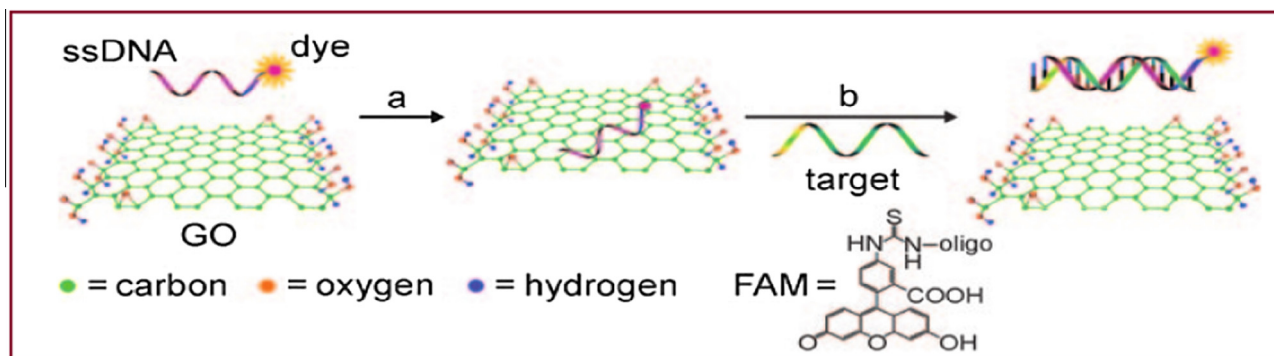


**Figure 6** Schematic representation of the target-induced fluorescence change of the ssDNA–FAM–GO complex (see text for details). FAM is the fluorescein-based fluorescent dye. Reproduced with permission Lu et al. (2009a, 2009b, 2009c).

interaction and hydrogen bonding have been attributed to the binding process (Manohar et al., 2008; Park et al., 2013; Huang and Liu, 2012).

The following mechanisms could be predicted for the hybridization of DNA on to the surface of GO (Liu et al., 2013a, 2013b) and have been schematically described in Fig. 7:

1. Langmuir–Hinshelwood mechanism: It is considered that fluorophore-labeled probe DNA is already adsorbed on the surface of GO which produces a dark background because of the quenching of fluorescence by GO. If this mechanism is followed then when complimentary DNA (cDNA) interacts with the probe DNA, a duplex is formed on the surface of GO which gets desorbed. This takes place in gas phase.
2. Eley–Rideal mechanism: This occurs in solution phase where probe DNA directly interacts with the cDNA.
3. Displacement mechanism: Some of the probe DNA is displaced by the cDNA to hybridize with the free DNA in the solution phase.

These mechanisms provide an insight into the GO/DNA system thereby leading to the rational engineering of biosensors with improved sensitivity and study of reaction dynamics in biomolecular systems. It is very important to understand these mechanisms for the applications in device fabrication, targeted drug delivery and imaging.

In double stranded (ds) DNA, the nucleotide bases are hidden in the helical structure. This prevents their effective interaction with the GO surface in contrast to ssDNA. For the detection of dsDNA, GO–organic dye ionic complex has been developed which involves the exchange of ions on the carboxylic acid groups adsorbed at the edges of GO (Chung et al., 2013). The efficient quenching ability of GO for different fluorophores is due to non-radioactive electronic excitation energy transfer from the fluorophore to GO and large cross

section area (Liu et al., 2014; Kim et al., 2010; Hong et al., 2012). The performance of GO based biosensor and fluorescence quenching of adsorbed dyes is also reported to be affected by C/O ratio of GO materials. The higher the ratio, abundant is the GO domains which in turn are responsible for fluorescence quenching and thus, greatly affecting the sensitivity and detection assay (Swathi and Sebastian, 2008).

One of the prominent features of GO to act as a weak acid cation resin in the presence of aromatic domain and functional groups to react with metal cations or positively charged organic molecules has enabled its coupling with readily available inexpensive and stable dyes to design novel biosensors (Huang et al., 2011). Wang et al. constructed a cost-effective electrostatic nanocomposite from Rhodamine 6G (R6G) and GO for selective detection of DNA. When negatively charged GO interacts with positively charged dye molecule, a charge transfer complex ( $R6G^+GO^-$ ) is formed which significantly quenches fluorescence. The complex formed had strong ionic and  $\pi$ - $\pi$  stacking interactions between  $R6G^+$  and  $GO^-$ . It was deduced that in the presence of DNA, the electrostatic noncovalent interaction between  $GO^-$  and  $R6G^+$  was disturbed and there was restoration of the fluorescence of complex. This was due to the competition to interact with R6G between GO and DNA. The fluorescence probe based on the formation of the above complex detected DNA in the presence of metal ions and macromolecules in biological fluid with excellent selectivity. This biosensor could be used for the detection of analytes through simple ion exchange process (Wang et al., 2012a, 2012b).

GO has paved its way in the formation of novel fluorescence biosensing strategy for simple, fast and sensitive selection of quadruplex-binding ligands (Mergeny et al., 2001). G-quadruplex are four-base-paired planar secondary DNA structures found in human telomeric (repetitive DNA sequences at the end of chromosomes) DNA. Quadruplex ligands interfere with proliferation of cancer cells and thus,

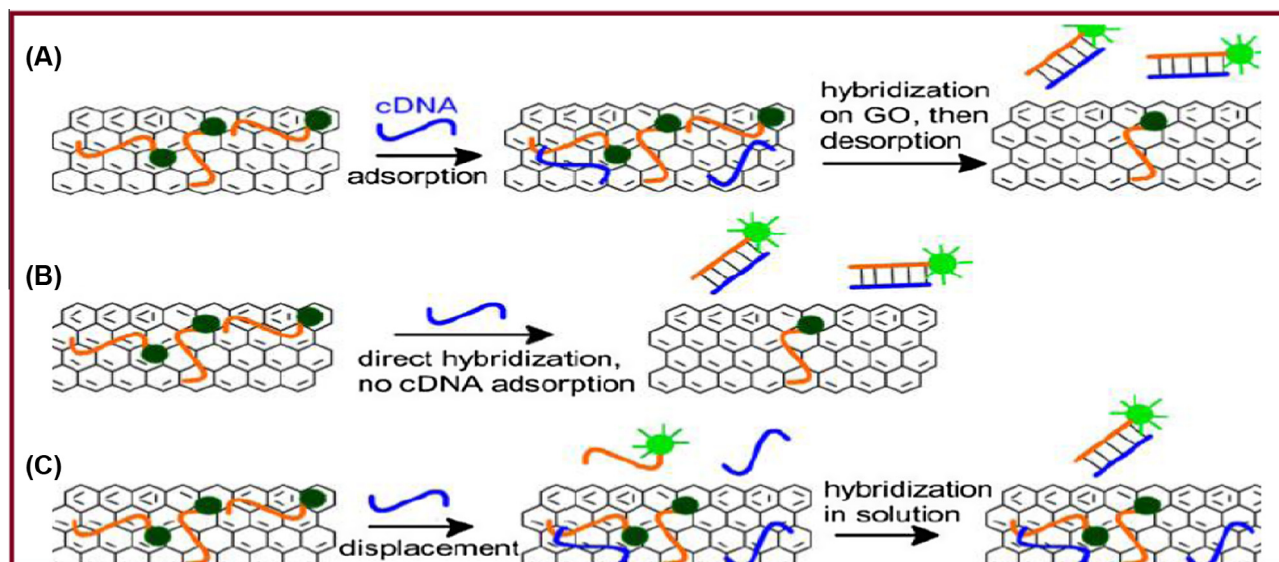


**Figure 7** The possible mechanisms for the hybridization of probe DNA adsorbed by GO and its cDNA (target DNA). In all the cases, the probe DNA with a fluorophore label is preadsorbed and the cDNA is added afterward. The tendency of GO adsorbing ds-DNA is lower than that of the adsorption of ssDNA. (A) Langmuir–Hinshelwood mechanism. (B) Eley–Rideal mechanism. (C) Displacement mechanism. Reproduced with permission Liu et al. (2013a, 2013b).

act as potential target for cancer therapy (Makarov et al., 1997). GO sheets are used for selecting these ligands. Because of the  $\pi$ - $\pi$  stacking between DNA bases and GO, FAM-labeled probe binds with GO surface thus, quenching the fluorescence of dyes. When these quadruplex binding ligands are added to GO, a quadruplex structure (Fig. 8) is formed from single stranded signal probe resulting in the release of DNA on GO surface and recovery of fluorescence (Wang et al., 2012a, 2012b). Among three medicinal Chinese ligands, flavonoid molecules acted as effective quadruplex binding ligands. These were found to possess low dissociation constant ( $K_d$ ) value with the signal probe and thus, induced high fluorescence recovery ( $F/F_0$  ratios  $\geq \sim 2$ ), where,  $F_0$  and  $F$  represent the fluorescence intensity of FAM-labeled signal probe/GO complex in the absence and presence of drugs.

### 5.2. Graphene oxide biosensors for the detection of glucose/ amino acids/vitamin/proteins/ATP

The turn on fluorescence sensing technique based on GO-DNA interaction has been used to sense molecules to different extent. Glucose is one of the very important molecules required for the normal growth of cell and requires continuous monitoring of blood sugar levels for the management of diabetes mellitus. In this regard, the GO-ssDNA interactions provide high selectivity for the determination of glucose in serum samples (Zhang et al., 2014). In the presence of glucose, its oxidation produces hydrogen peroxide ( $H_2O_2$ ) which in the presence of ferrous ions ( $Fe^{2+}$ ) generates hydroxyl radical through the Fenton reaction (Yang et al., 2013a, 2013b). This hydroxyl radical causes the oxidative damage of DNA by abstracting hydrogen from the deoxyribose phosphate backbone (Liu et al., 2011a, 2011b, 2011c; Wang et al., 2008a, 2008b). As a result, FAM-labeled long ssDNA is cleaved into FAM-linked DNA fragment which is released from the graphene surface due to the weak interaction between GO and FAM-linked DNA fragment, and the fluorescence of the system increases (Li et al., 2012a, 2012b). In the absence of glucose, no change is seen as Fenton reaction does not occur since there is no generation of hydrogen peroxide. Thus, ssDNA is not damaged since it is bound to GO surface through  $\pi$ -stacking interactions. As labeled FAM and GO come close, the fluorescence of FAM is quenched via fluorescence-resonance energy transfer (FRET). Hence, as the concentration of glucose increases in the system, there is

gradual increase in fluorescence intensity of the system (Fig. 9A).

The inset of Fig. 9B depicts the strong fluorescence (FL) emission of FAM-labeled ssDNA which was quenched after the addition of GO indicating the adsorption of ssDNA on the GO surface. After the addition of glucose there was restoration of FL of DNA-GO system and generation of hydroxyl radical through Fenton's reaction which caused the cleavage of ssDNA into short FAM-labeled DNA fragment. Due to the weak interaction of this short fragment of DNA with GO, enhancement of fluorescence was observed. In the absence of glucose oxidase no change in fluorescence was observed indicating that the presence of enzyme was necessary in order to sense glucose by DNA-GO system.

Functionalized GO has also been used for glucose detection (Song et al., 2010). The covalent attachment of carboxylic groups of GO with the amine of glucose oxidase results in the formation of an efficient enzyme electrode acting as a biosensor. The modification of electrodes with GO increases interfacial electron transport. This is attributed to the different functionalities present in GO. The immobilization of enzymes on the electrode surface retaining its biological activity is one of the crucial steps in the fabrication of excellent biosensors. The selectivity of the electrodes can be enhanced toward glucose oxidase enzyme by modifying it with Prussian blue (PB) which acts as a redox mediator by catalytically reducing hydrogen peroxide ( $H_2O_2$ ) in the solution. Further, the use of GO on the PB modified electrode increases the catalytic current and stability. Hence, it provides a biocompatible environment for the sensitive detection of glucose exhibiting broad linearity, excellent reproducibility and storage stability (Vinu Mohan et al., 2013).

The demand for enzyme free based biosensors has increased rapidly for advanced blood sugar detector, controlled food preparation processes and glucose detection with high sensitivity, selectivity and fast response. Electrochemical glucose sensors are categorized as (a) glucose oxidase (GOD) based (b) enzyme free glucose sensing. GOD based sensors suffer from reproducibility and stability issues; therefore, more focus is primarily on enzyme free sensors. The advancement in field of synthesis of nanoparticles (NPs) has paved a way for enzyme free glucose biosensors. Special emphasis is on transition metal oxide nanoparticles (NPs). Cobalt oxide ( $CoO_x$ ) nanoparticles-GO heterostructures amplify the signals for glucose detection and provide a green and reproducible method

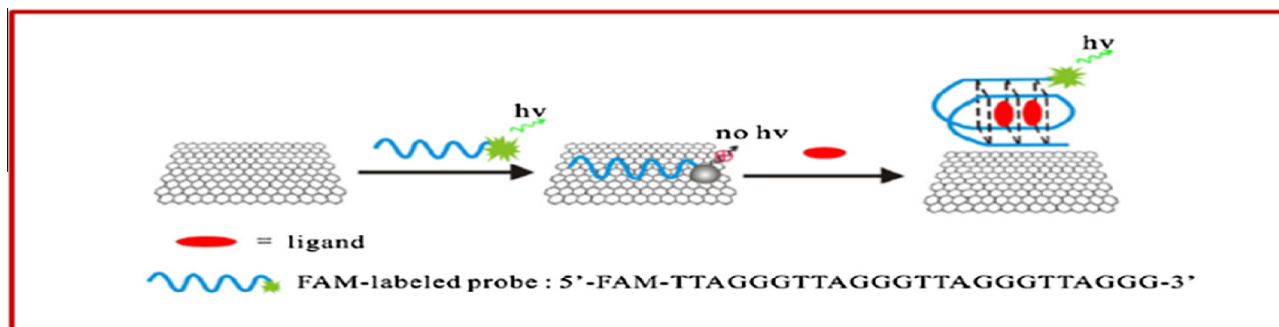


**Figure 8** Schematic illustration of the screening of quadruplex-binding ligand based on graphene oxide biosensing platform. Reproduced with permission Wang et al. (2012a, 2012b).

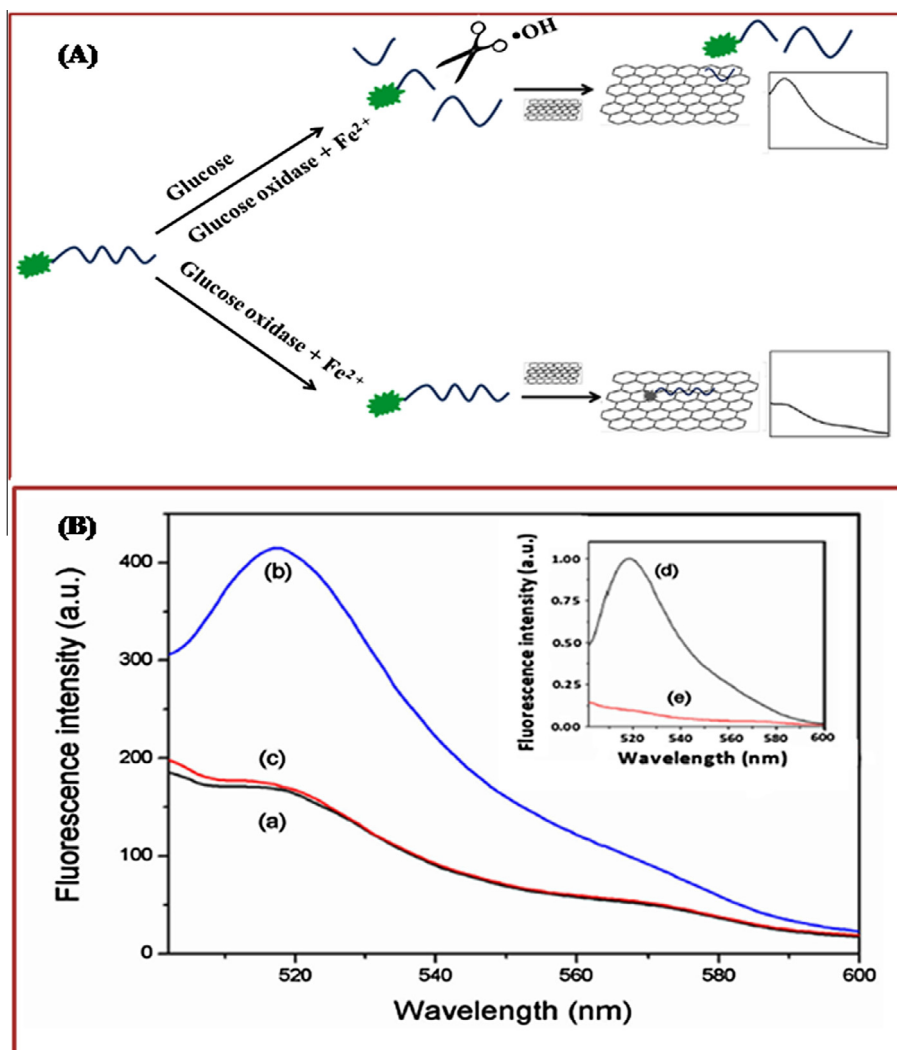
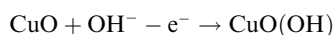


**Figure 9** Schematic illustration of (A) fluorescence turn-on determination of glucose based on GO–DNA interaction, (B) fluorescence emission spectra of FAM-labeled ssDNA under different conditions: (a) GOx + GO + DNA; (b) glucose + GOx + GO + DNA; (c) glucose + GO + DNA. The inset shows the fluorescence quenching of FAM labeled ssDNA before (d) and after introduction of GO. Reproduced with permission Zhang et al. (2014).

for the development of biosensors for enzyme free detection of glucose. They adhere to the surface of GO making electron transfer process convenient and improve the detection sensitivity (Li et al., 2014a, 2014b; Ding et al., 2010; Xiang et al., 2013). CuO NPs based GO biosensors have been reported to be prepared by hydrothermal method for non-enzymatic biosensing of glucose. The NPs were loaded in GO sheets and the sensing properties of CuO NPs were found to be improved when loaded in GO sheets. This has been attributed to better electrochemical activity and promotion of electron transfer reactions (Song et al., 2013). According to electrochemical behavior a redox couple (Cu II/Cu III) is formed which is very important for the non-enzymatic electrochemical detection of glucose and the reaction is



Once, glucose is injected, the following oxidation reaction takes place:



Fig. 10 explains the non-enzymatic glucose sensing mechanism by CuO NPs/GO composite.

In view of the immobilization of enzyme which is one of the important aspects for the construction of any biosensor, a nanocomposite matrix based on ferrocene (Fc)-branched organically modified silica material (ormosil)/chitosan (CS)/graphene oxide (GO) was fabricated acting as an excellent glucose biosensor. Glucose oxidase is negatively charged in the physiological media and can be easily immobilized on Fc-conjugated ormosil/CS/GO nanocomposite material via self-assembly and sol-gel technology. The dispersion of GO within the Fc-branched ormosil/chitosan CS matrix improves the stability of GO and the conductivity of matrix film thereby facilitating the electron transfer between the mediator and the electrode (Peng et al., 2014). For effective electron transfer and sensitive detection of molecules, mediator is necessary for biosensors. In this case, ferrocene acts as a mediator which is conjugated with silica material (ormosil) to prevent leakage and enhance stability.

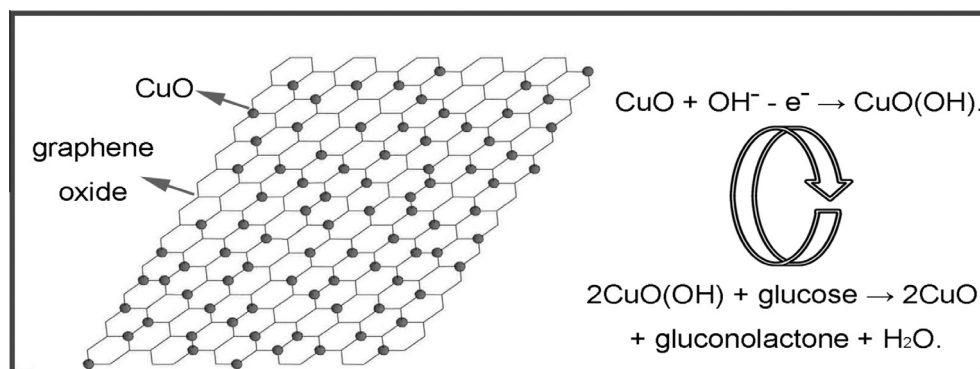


**Figure 10** Non-enzymatic glucose sensing mechanism of CuO NPs/GO composite. Reproduced with permission Song et al. (2013).

Shamsipur and Tabrizi designed an electrochemical biosensor composed of electrochemically reduced graphene oxide (ERGO) and sodium dodecylsulfate (SDS) using single step reduction of GO for the detection of glucose. SDS was found to increase the immobilization of glucose oxidase on ERGO surface due to its excellent ability to form film. The detection limit of the biosensor was found to be  $40.8 \mu\text{M}$  at a signal-to-noise ratio of 3 (Shamsipur and Tabrizi, 2014). The results of this biosensor were similar ( $\pm 5\%$ ) to those obtained from clinical analyzer.

Bimetallic nanoparticles have become an area of prominent research and used as electrocatalysts. Each component retains its functional properties and results in enhanced surface area, electron transfer and improved biocompatibility. Among different metals, Pt and Pd are the two most electrocatalytic metals. Hossain and Park immobilized glucose oxidase enzyme on the reduced graphene oxide (RGO) surface deposited with PtPd NPs for glucose detection. This hybrid electrode had high catalytic activity toward the oxidation (response time of 3 s, sensitivity  $486 \times 10^{-6} \text{ A/mM cm}^2$ , linear range 0.5–6.5 mM) and reduction (response time of 2 s, sensitivity  $814 \times 10^{-6} \text{ A/mM cm}^2$ , linear range 0.5–8 mM) of hydrogen peroxide (Hossain and Park, 2014). The FTIR spectra of GO depict major peaks at  $3410.0 \text{ cm}^{-1}$ ,  $1709.4 \text{ cm}^{-1}$ ,  $1629.5 \text{ cm}^{-1}$ ,  $1382.2 \text{ cm}^{-1}$  and  $1080.6 \text{ cm}^{-1}$ , corresponding to –OH stretching, C=C stretching, –OH bending of adsorbed water molecule, aromatic C=C, deformation vibration of –OH and C–O stretching vibration of alkoxy groups, respectively (Fig. 11A) (Khali et al., 2012; Shen et al., 2010). The peaks at  $3421.7 \text{ cm}^{-1}$ ,  $1718.5 \text{ cm}^{-1}$ ,  $1624.2 \text{ cm}^{-1}$ ,  $1577.7 \text{ cm}^{-1}$  and  $1419.9 \text{ cm}^{-1}$  corresponded to RGO arising from –OH stretching, C=O stretching, –OH bending, C=C stretching and deformation of –OH vibration, respectively (Wang et al., 2011a, 2011b; Szabo et al., 2005). Fig. 11B and C shows the XPS spectra of GO and RGO, respectively. A considerable degree of oxidation has been depicted corresponding to the carbon atoms in different functional groups. A new peak at  $285.7 \text{ eV}$  arises after the reduction of GO showing C–C bonds (Park et al., 2013). The reduction of oxygen atoms on the surface during the reaction and heat treatment created RGO. The high sensitivity and stability of the electrode contribute in the construction of a practical glucose biosensor which could be extended to the immobilization of the other biomolecules.

One of the challenging tasks is the determination of amino acids in biological fluids. Though different methods are

available such as surface enhanced Raman scattering (SERS), high performance liquid chromatography (HPLC), luminescence and fluorescence these have complicated protocols for sample preparation and processing (Cheng et al., 2011; Razmi et al., 2011; Sánchez-Machado et al., 2008; Ma et al., 2011). Electrochemical methods are preferred because of their sensitivity, accuracy, simplicity and lower cost. An electrochemical biosensor based on GO and MWCNTs could detect catalytic oxidation of L-tyrosine. This amino acid is very important for human nutrition and is needed for maintaining a positive nitrogen balance. Its absence can cause albinism whereas higher concentration levels result in sister chromatid exchange (Zhu and Xu, 2010). The high sensitivity of the biosensor is due to the improved electrical conductivity of GO and high surface area of MWCNTs which improves the electron transfer. Secondly, there is a  $\pi$ – $\pi$  stacking between GO and aromatic structure of L-tyrosine (Li et al., 2013a, 2013b). The mechanism for the electrochemical oxidation of L-tyrosine is explained from the cyclic voltammetry (CVs) graphs in Fig. 12. Voltammetric response indicates the oxidation of  $10.0 \mu\text{M}$  L-tyrosine at GO/MWCNTs/GCE as there is linear increase of peak current ( $I_{pa}$ ) with the scan rate ( $\nu$ ) in the range of  $20$ – $250 \text{ mV s}^{-1}$ . This is found to be adsorption controlled electrode process. The linear regression equation is expressed as  $I_{pa} (10^{-5} \text{ A}) = 0.01775\nu (\text{mV s}^{-1}) + 0.4220x$  ( $R^2 = 0.9967$ ).

As the scan rate for the oxidation of L-tyrosine progresses, peak potential ( $E_{pa}$ ) is shifted toward more positive values thereby indicating irreversible electrode process. Laviron's equation defines the adsorption-controlled and irreversible electrode processes

$$E_{pa} = E^\circ + (RT/\alpha nF) \ln(RTk^\circ) + (RT/\alpha nF) \ln \nu$$

where  $\alpha$  is the electron transfer coefficient,  $k^\circ$  is standard heterogeneous rate constant of the reaction,  $n$  is the transferred electron number,  $\nu$  is the scan rate and  $E^\circ$  is the formal redox potential (Laviron, 1974). Thus, this voltammetric method has been found to be excellent for the determination of L-tyrosine in human blood serum and urine samples. It is more efficient as compared to methods where sample pretreatment is one of the difficult tasks.

A very attractive strategy to create binding sites for some specific molecules is molecular imprinting technique. Though GO has been used in conjugation with quantum dots (QDs) for enhanced photocurrent and photocatalysis electrochemical sensing very little attention has been given for the sensing of

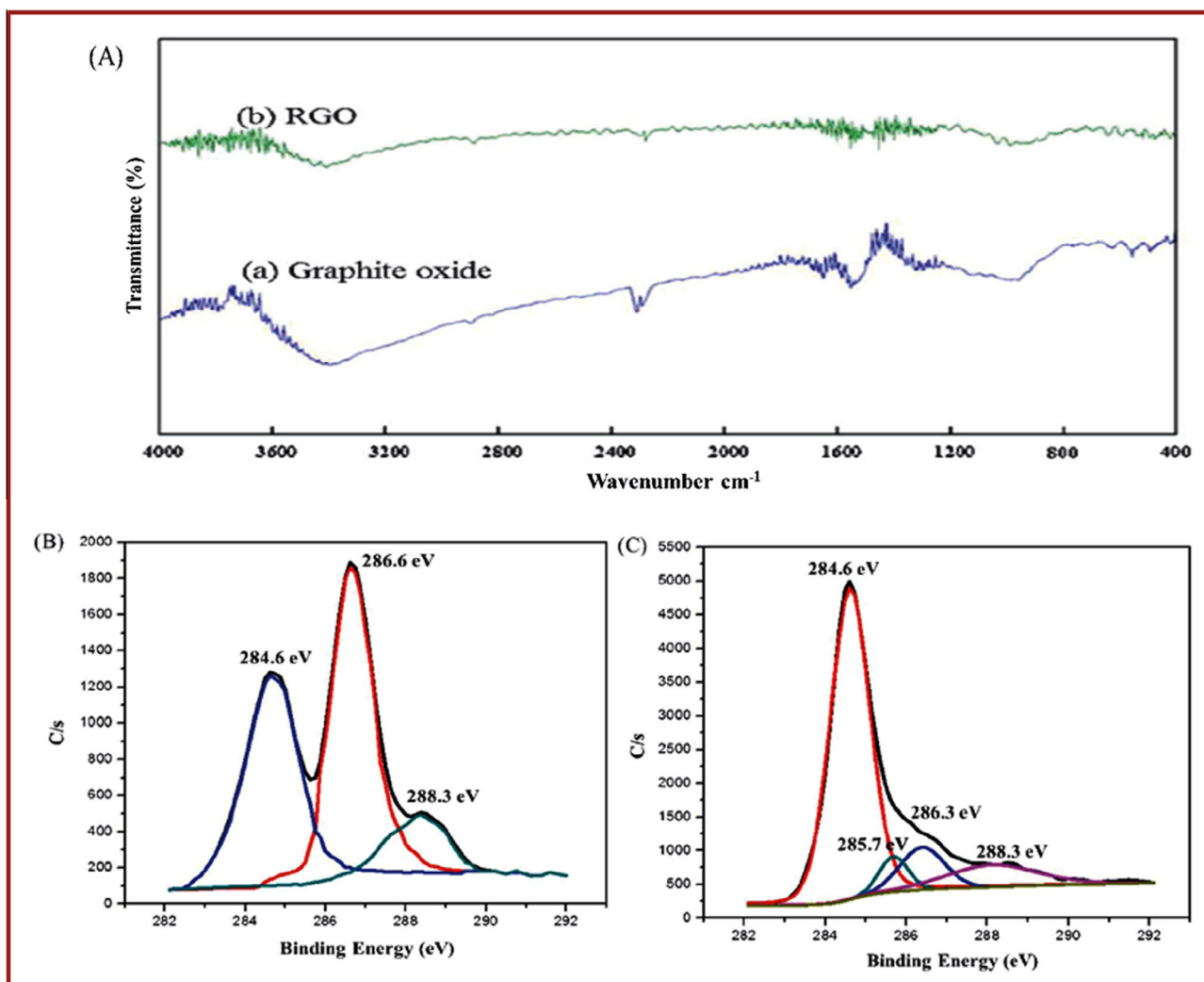


**Figure 11** FTIR spectra of (A) graphite oxide and RGO, XPS spectra of (B) graphite oxide and (C) RGO. Reproduced with permission Hossain and Park (2014).

some biomolecules such as vitamins. The fluorescence intensity of GO is quenched in the presence of UV radiations; therefore, ionic liquids (ILs) are introduced on the surface of GO as these provide surface binding groups between GO and QDs. Molecular imprinted polymers (MIPs) have been reported to be combined with ILs to fabricate GO/QDs composite biosensor for the detection of trace levels of vitamin E in real samples. It is an antioxidant that protects living cells by quenching free radicals (Liu et al., 2013a, 2013b). The UV-visible spectrum (Fig. 13A) of MIP and vitamin E explains the binding mechanism. MIPs have been found to possess better photochemical stability when compared to isolated single QDs or GO. Fig. 13B indicates the conduction band of MIP to be close to that of vitamin E. Thus, charges could be easily transferred to the lowest unoccupied orbitals of vitamin E resulting in the fluorescence quenching between the two. The energy transfer is a possible mechanism for the fluorescence quenching owing to no spectral overlap between the absorption spectrum of vitamin E and emission spectrum of MIP. The fluorescence intensity of MIP was found to decrease with the increasing concentration of vitamin E in the range of  $2.30 \times 10^{-2}$ – $9.20 \times 10^2$   $\mu\text{M}$  with the detection limit of 3.5 nM.

Based on effective sensing of biomolecules by fluorescence energy transfer (FRET) from QDs to GO, Dong et al. developed a novel sensitive and selective biosensor. QDs were used as fluorophore to label MB (molecular beacon, single stranded oligonucleotide hybridization probe) and enhance its detection sensitivity. MB could be substituted with any other aptamer (thrombin binding) for the detection of proteins (Dong et al., 2010). The fluorescence intensity ratio is given by the Stern–Volmer equation (Li et al., 2010a, 2010b):

$$F_0/F = 1 + K_{SV}[\text{VE}]$$

where  $F_0$  and  $F$  are the fluorescent intensities in the absence and presence of biomolecule/analyte,  $K_{SV}$  is Stern–Volmer constant and  $[\text{VE}]$  is the quencher concentration. Fig. 14 shows the fluorescent intensity ratios of thrombin with different concentrations on addition of GO. It is observed that as the concentration of thrombin increases, the ratio increases linearly indicating that this approach could be applied potentially to other proteins also.

Recently, a very interesting approach was designed to fabricate graphene based impedance sensors where protein molecules were directly adsorbed on the surface of reduced

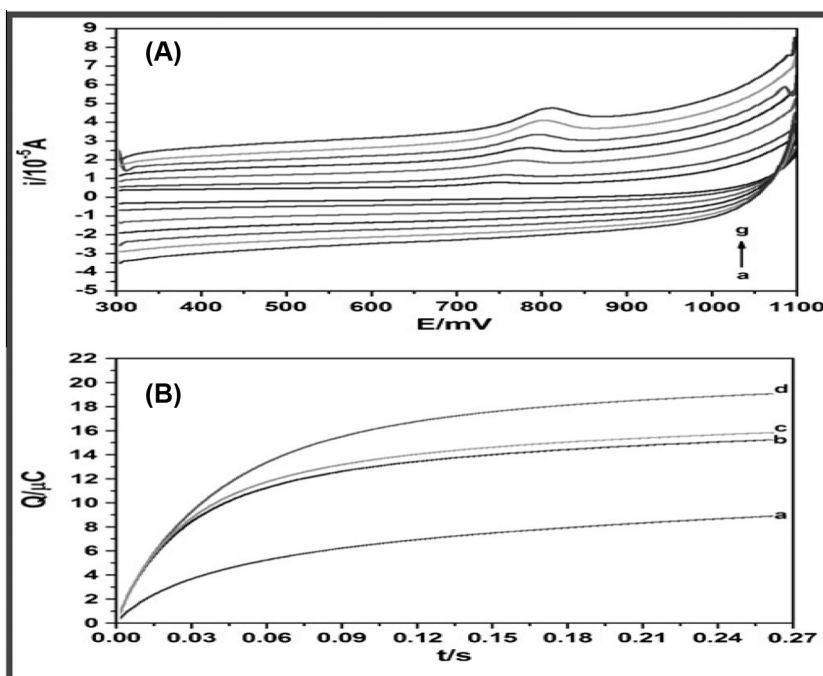


**Figure 12** CVs of 10.0  $\mu\text{M}$  tyrosine at GO/MWCNTs/GCE with different scan rates (a  $\rightarrow$  g: 20, 40, 80, 120, 160, 200, 250  $\text{mV s}^{-1}$ ); b Chronocoulograms for GCE (a), MWCNTs/GCE (b), GO/GCE (c) and GO/MWCNTs/GCE (d) in 0.1 mM  $\text{K}_3[\text{Fe}(\text{CN})_6]$ ; (pulse range: 300–1100 mV; pulse width: 0.25 s). Reproduced with permission Li et al. (2013a, 2013b).

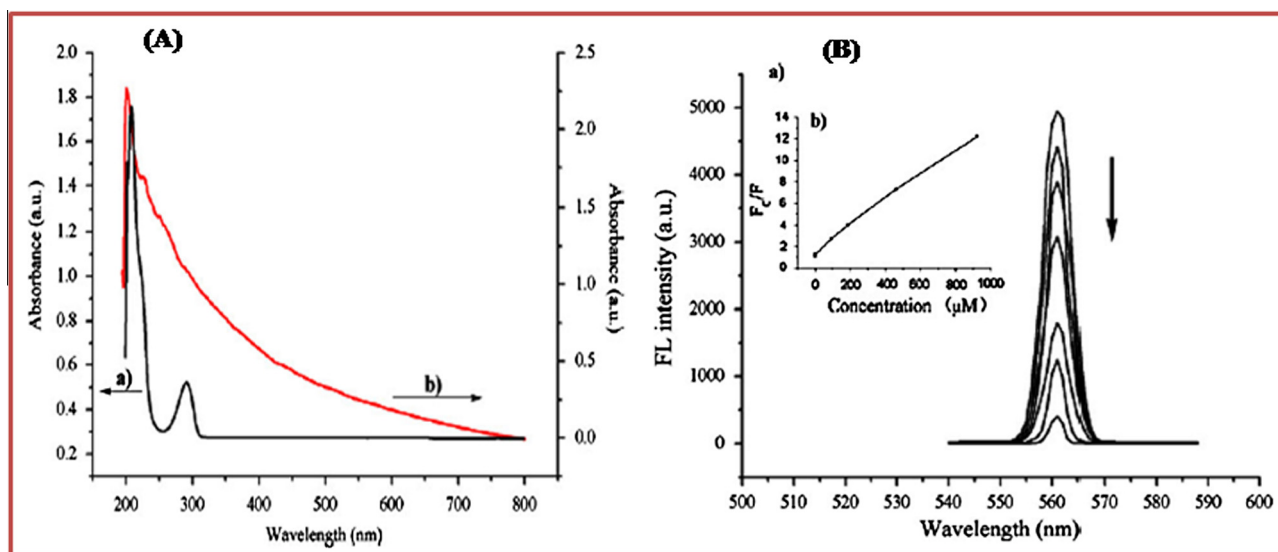


**Figure 13** (A) UV-visible spectra of (a) vitamin E solution (b) MIP, (B) fluorescence spectra of (a) MIP with increasing con. of vit E (b) effect of vit E conc. on the fluorescence intensity of MIP. Reproduced with permission Liu et al. (2013a, 2013b).

graphene oxide (rGO) thin films without the need of pre-functionalization of GO. The denatured proteins adsorbed on the surface of rGO through  $\pi$ -stacking interactions. The rGO sheets were prepared by the spin assisted layer-by-layer (LbL) assembly method followed by thermal reduction process. Denatured bovine serum albumin (BSA) was used as a model probe to enable its direct adsorption on the surface of rGO. The data obtained from electrochemical impedance spectroscopy (EIS) reveal that electrochemical properties of LbL-assembled rGO films can be tuned by varying the number

of bilayers. As the deposition number increases, interfacial charge transfer resistance ( $R_{ct}$ ) values decrease due to the flow of charge through randomly formed networks within the stacked rGO nanosheets. Fig. 15 shows the formation of deformed semicircle in the case of single bilayer resulting in irregularly defined  $R_{ct}$  due to incomplete coverage of nanosheet.  $R_{ct}$  can be measured directly as semicircle diameter. Subsequent addition of bilayers produces consistent, stable and smaller values of  $R_{ct}$  as the full surface is covered uniformly. In this study, 2 layers were considered to be optimum

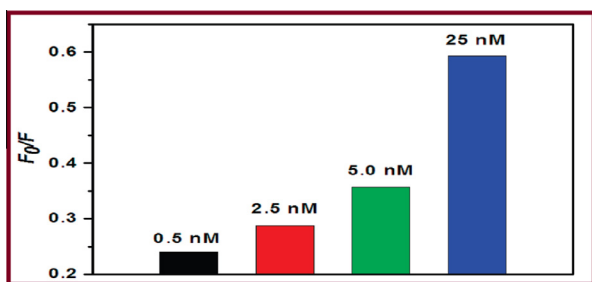


**Figure 14** Fluorescence intensity ratio  $F_0/F$  for aptamer-QDs (50 nM) after incubation with thrombin at different concentrations and then addition of GO (0.1  $\mu\text{g/mL}$ ) for 5 min. Reproduced with permission Dong et al. (2010).

to have a uniform  $R_{ct}$  value and maintain surface roughness (Kim et al., 2013a, 2013b).

Loo et al., adopted solid state electrochemistry to develop a unique biosensing protocol involving graphene oxide nanoplatelets (GONPs) of dimensions  $50 \times 50$  nm for the aptasensing of protein thrombin in the concentration range of 3 pM–0.3  $\mu\text{M}$  (Loo et al., 2013a). Thrombin aptamer (THR-APT-15) was immobilized on the electrode surface and then this modified electrode was exposed to thrombin protein. The two case studies were carried out to detect the sensitivity of the biosensor. In the first case, the modified electrode was exposed to thrombin and incubated in the solution containing GONPs. Here, it was observed that thrombin bound to aptamer and resulted in its partial removal due to the conformational changes occurring as a result of the binding of protein and the aptamer. In the next step, GONPs bound to the remaining immobilized THR-APT-15 via strong  $\pi$ - $\pi$  interactions. This led to the reduction peak signal of greater magnitude as compared to the second case where modified electrode was incubated directly in GONPs solution. Thus, it was concluded that as there is partial removal of immobilized aptamer on binding with thrombin, it provided large electrode surface available for charge transfer and resulting in greater reduction potential. Hence, GONPs served as excellent electroactive label for sensing of thrombin protein with greater sensitivity and selectivity. Loo and coworkers did similar novel work on the same lines as discussed above

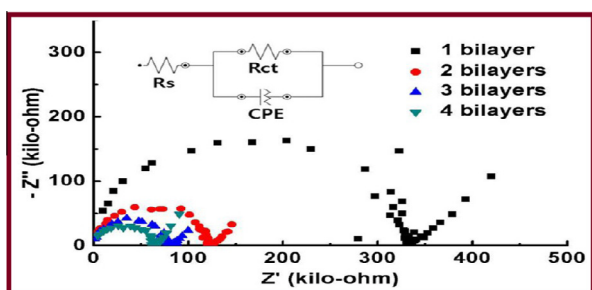


**Figure 15** Normalized Nyquist plot of rGO films with varying bilayer deposition numbers from 1 to 4. (Inset) Equivalent circuit used in a conventional three-electrode system without redox probes ( $R_{ct}$  charge transfer resistance, CPE constant phase element,  $R_s$  electrolyte solution resistance). Reproduced with permission Kim et al. (2013a, 2013b).

where they employed GONPs as labels for protein target molecule (biotin–avidin recognition). The strategy was based on use of biotinylated DNA probe to be immobilized on the electrode surface rather than that of simple biotin probe. Due to high surface area of GONPs, they served as excellent biosensor with high sensitivity (Loo et al., 2013b).

GO has shown a great potential for use as biosensors due to its surface modification versatility, good water dispersibility and photoluminescence but there are limited studies on GO-based surface plasmon resonance (SPR). Human immunoglobulin G (IgG) is a protein complex composed of four peptide chains and represents 75% of serum antibodies in humans. GO-based SPR biosensor has been fabricated for its detection. It is noticed that there is a greater change in the refractive index when GO is fabricated on the gold film surface of a SPR biosensor. The surface plasmon wave is affected by the changes in the refractive index when human Ig is coupled with gold nanorods (Zhang et al., 2013).

To explore the protein functions in the biological systems, sensing and imaging of molecules inside living cells has emerged as a powerful tool. ATP and GTP are biological process regulating molecules. Therefore, their detection is desirable in visualization of living cells which is one of the major challenges in the field of molecular imaging. The limitation of presently used artificial probes is their ability to penetrate inside the cell membrane. Graphene oxide nanosheets (GO-nS) have proved to be efficient probes for the detection of ATP inside living cells due its excellent features: (i) cell-membrane permeability, (ii) low toxicity, and (iii) sensitive detectability by confocal microscopy (Nel et al., 2009). For biological applications of aptamers, protection from enzymatic cleavage is a key step. Aptamer/GO-nS has been designed for the first time for in-situ molecular probing in living cells as shown in Fig. 16 (Wang et al., 2014).

Adenosine triphosphate (ATP) is a major energy carrier which not only plays an important role in the signal of pathways and control of diseases but also is an indicator of cell viability and its condition. Different methods have been reported in the literature for the determination of ATP but there is a need to develop simple, selective and sensitive techniques for pathological and clinical diagnosis. Due to high quenching efficiency of GO, it shields attached biomolecules from degradation or enzymolysis (Lu et al., 2010). The large surface area enables effective loading of proteins, nucleic acids and small inorganic molecules via  $\pi$ -stacking interactions or chemical modifications (Wu et al., 2012; Yin et al., 2013a, 2013b). Therefore, GO is being widely explored and used for sensing applications. Ning et al., designed a novel fluorescent aptamer based on noncovalent assembly of a label free detection probe and GO. The probe was adsorbed on the GO surface by  $\pi$ - $\pi$  stacking and no fluorescence was observed. But in the presence of ATP and complimentary DNA (cDNA) of the signal probe, significant fluorescence was observed due to the intercalation of cDNA with SYBER Green I (Fig. 17). The fluorescence was found to increase in the presence of ATP (Ning et al., 2014).

### 5.3. Role of graphene oxide based biosensors in food safety

Food safety is upcoming area of science which involves handling, preparation and storage of food to prevent food borne

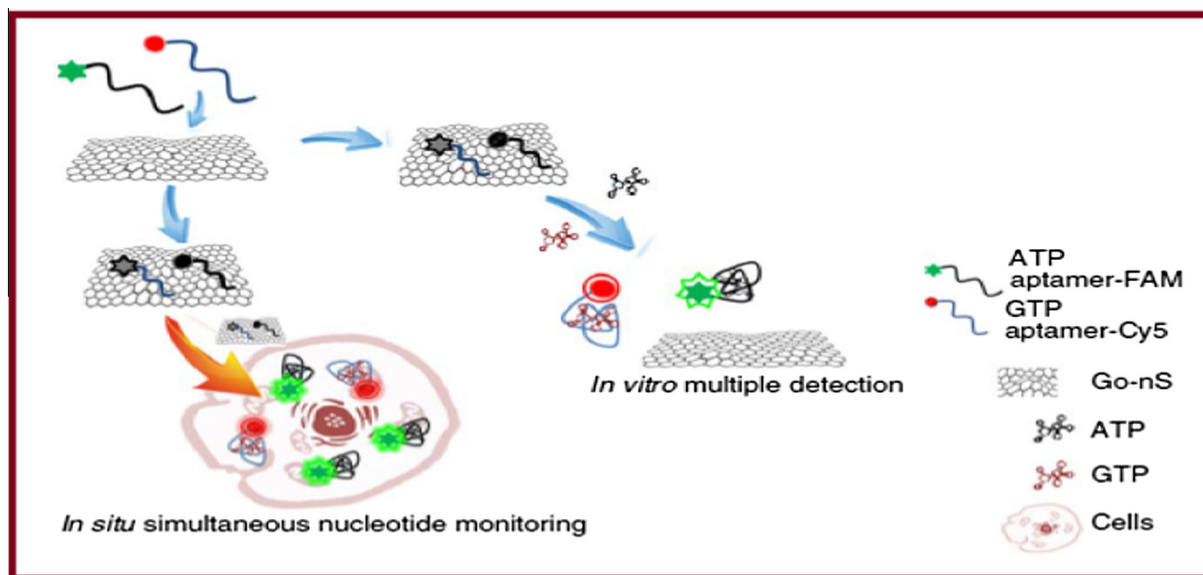


**Figure 16** Schematic representation of in vitro and in-situ molecular probing in living cells by using the aptamer/GO-nS nanocomplex. Reproduced with permission Wang et al. (2014).

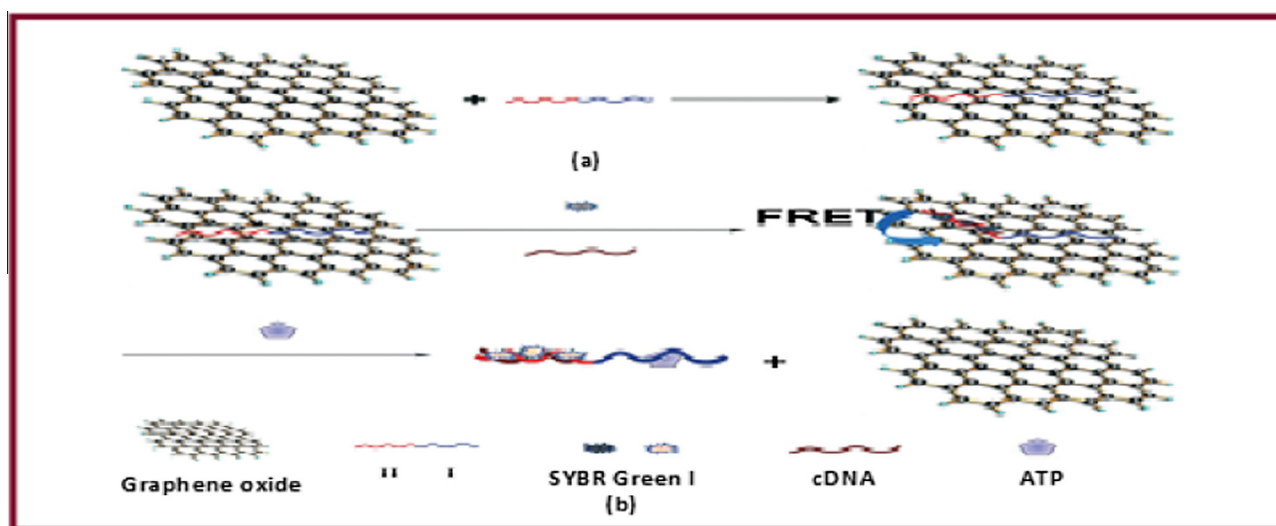


**Figure 17** Schematic representation of the probe/GO platform for ATP determination (a) preparation of probe/GO complex and (b) enhancement of fluorescence upon addition of ATP and complimentary DNA. Reproduced with permission Ning et al. (2014).

diseases. Unsafe food is responsible for causing many diseases from diarrheal to different forms of cancer (Millour et al., 2011). Hydrogen peroxide ( $H_2O_2$ ) is a powerful oxidizing agent which is used as an antimicrobial agent in the food packages. However, its use should be limited since above 3% of the  $H_2O_2$  solutions leads to vomiting, irritation to mucosa, burning in mouth and stomach, etc. Thus, its detection in food samples is very important. The two-dimensional (2D) honeycomb lattice of reduced GO holds a great potential for biosensor applications as it allows the fast movement of electrons for different electroactive species when employed as an electrode substrate (Cheng et al., 2012; Walcarius et al., 2013). GO based aptamers have now been developed for the detection and analysis of food borne pathogens. Aptamers are single stranded DNA or RNA molecules that can bind to pre-selected targets including proteins and peptides with high affinity and

specificity. They bind to GO by  $\pi$ - $\pi$  stacking interaction, as a result of which fluorescence of aptamer is quenched due to fluorescence resonance energy transfer (FRET). This type of biosensor can detect bacteria in a very short time. Duan et al. synthesized aptamer based on GO and labeled with fluorophore (5-carboxyfluorescein) for the detection of *Salmonella typhimurium*, food borne pathogen. This pathogen causes diarrheal diseases posing a major health threat in developing countries. It was observed that aptamer could detect *S. typhimurium* with high specificity and no cross reaction with other pathogens (Plym Forshell and Wierup, 2006; Duan et al., 2014). The rapid detection is based on turn-on/turn-off fluorescence which is a dynamic process.

The fluorescence of QDs is greatly quenched by GO. This is employed in the designing of sensors which can detect mycotoxins in trace levels in food items. Certain genre of fungi

releases mycotoxins which are toxic in nature and contaminate agriculture food stock. They are carcinogenic and cause adverse health effects (Schenze et al., 2012; Richard et al., 2007). In another study, easily producible and cost-effective aptamers have been used as an alternative to antibodies for the detection of mycotoxins. They are combined with nanomaterials such as QDs for electrochemical measurements (Kashefi-Kheyraadi and Mehrgardi, 2012). The fluorescence from CdTe QD is quenched in the presence of GO and has detected carcinogenic mycotoxin (Aflatoxin B1) with high efficiency present in peanut oil as shown in Fig. 18 (Lu et al., 2015). In the absence of aflatoxin B1 (AFB1) in the system, aptamer present in QD-conjugate allows the adsorption of conjugates on GO nanosheet surface and results in QD fluorescence quenching, whereas, in the presence of AFB1, target is recognized by QD-attached aptamer forming well folded AFB1-aptamer complex. The nucleotide bases (purine and pyrimidine) present in aptamer which interact with GO through  $\pi$ -stacking are occupied by AFB1. Hence, conjugates are not able to attach to GO nanosheets and fluorescence is recovered.

In-situ synthesis of gold nanoparticles (Au NPs) on the surface of GO acts as a biosensor for the amperometric detection of hydrogen peroxide ( $H_2O_2$ ) in food items with improved analytical properties. Here, catalase was immobilized on the surface of Au NPs attached to GO modified glassy carbon electrode (GCE). Cyclic voltammetry studies showed that the background current increased in the presence of Au NPs. The couple of redox peaks were obtained at  $-170$  mV and  $-120$  mV after the conjugation of threonine-conjugated catalase molecules assembly on Au np/GO/GCE surface. The conductivity of GO was improved in the presence of Au NPs which was attributed to the fact that Au NPs acted as intervening 'spacer matrix' to penetrate through the GO sheets (Zhang et al., 2011a, 2011b).

#### 5.4. Graphene oxide biosensor for the detection of virus

Herpes simplex virus (HSV-1) is the most common pathogen infecting 70–90% of the world human population. Humans are the natural hosts of this virus where it causes infections at the epithelial cell level and neurons of the peripheral nervous system (Liashkovicha et al., 2011). The glycoproteins form the outer boundary of virus. gB and gC glycoproteins mediate the

entry of HSV-1 into host cells by binding to heparan sulfate (HS) proteoglycans. HS is negatively charged linear polymer playing role in cancer, amyloid diseases, infectious and inflammatory conditions. The virus binding to HS serves as the mechanism for the increase in the concentration of virus on the cell surface (Subramanian and Geratgthy, 2007; Choudhary et al., 2011). GO and partially reduced sulfonated graphene oxide (rGO-SO<sub>3</sub>) inhibit HSV-1 infections through a mechanism of competitive inhibition. Due to the presence of negatively charged groups on GO and rGO-SO<sub>3</sub>, similar to that present on HS, these mimic the cell surface of the virus thereby stopping the infection (Sametband et al., 2014). The cytotoxic tests revealed that GO and rGO-SO<sub>3</sub> were not toxic to cell cultures (vero cells) and also did not affect the cell's life cycle. In the upcoming future, the intrinsic properties of GO can be exploited for the development of antiviral surfaces.

Hepatitis C virus (HCV) is a single stranded RNA virus infecting 180 million people around the world causing chronic liver damage and hepatocellular carcinoma (Brody, 2011). Currently, no vaccine or effective therapy is available for hepatitis virus. Among different approaches adopted for the development of anti-HCV agent, DNAzyme (deoxyribose, Dz) is the upcoming therapeutic agent for the cleavage of HCV gene and subsequently preventing viral replication in human host cells (Chung et al., 2013). Nano-graphene oxide (nGO) based system has been reported for the intracellular delivery of Dz which targets mRNA of HCV nonstructural gene 3 (NS3) in human liver cells and prohibits gene replication (Fig. 19). The N-terminal of NS3 protein plays a vital role in HCV replication, and its inhibition can stop HCV from replicating. The nucleotide base of Dz binds effectively with nGO. As a result, the fluorescence from the dye attached to the 5' end of Dz is quenched. In the presence of the target sequence, there is double helix formation of Dz which causes the detachment of Dz from nGO surface followed by the cleavage of HCV NS3 RNA target sequence. This leads to the recovery of the fluorescence (Kim et al., 2013a, 2013b).

#### 5.5. Graphene oxide biosensors for the detection of different analytes

The functionalization of GO is done for the detection of drugs. Carboxyl functionalized GO modified electrode has detected non-steroidal anti-inflammatory drug, diclofenac (DCF) in

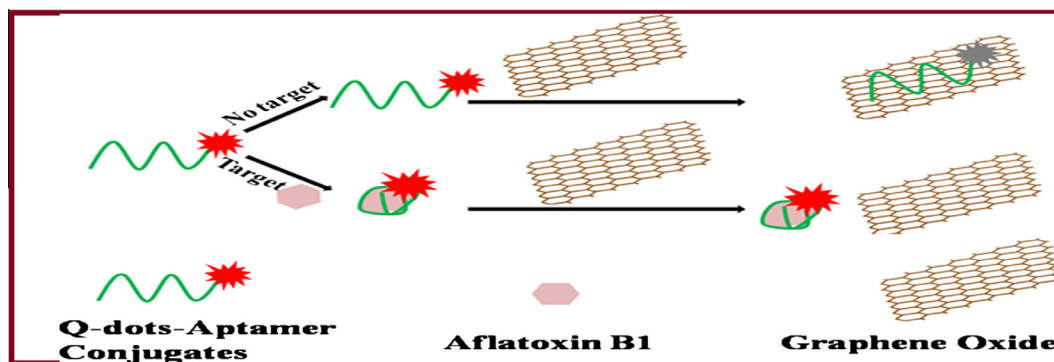


**Figure 18** Schematic illustration of fluorescent assay for AFB1 based on Q-dots-aptamer-GO quenching system. Reproduced with permission Lu et al. (2015).

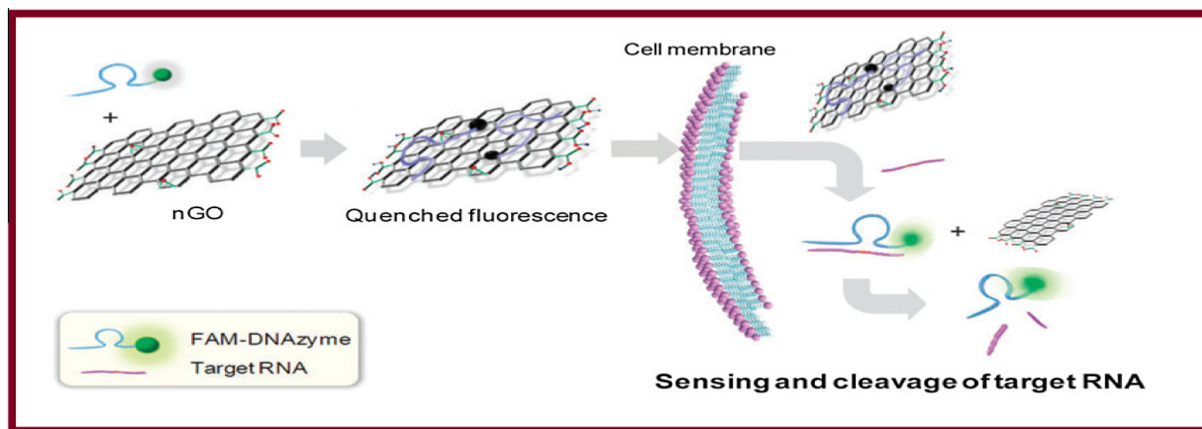


**Figure 19** Strategy of detection and knockdown of the target gene in mammalian cells based on Dz and nGO. Reproduced with permission Kim et al. (2013a, 2013b).

human urine and serum samples (Karuppiyah et al., 2015). This drug is widely used for the treatment of tuberculosis and urinary tract infections and has fewer side effects. Though many chromatographic and spectroscopic techniques have been used for the drug detection they are not rapid and require extensive sample preparation. The electrochemical technique employing functionalized GO is user friendly, cost effective and moreover a sensitive technique.

GO based biosensors are also used to determine analytes which are hazardous to the living environment. These include explosives, toxins and pesticides. Because of the presence of the hydroxyl groups in the center and carboxy groups at the edges, the functionalization of graphene oxide sheets can be done either by covalent or by non-covalent bonding. This improves the mechanical interactions between the sheets thereby improving the physical properties. The present world is facing threat to the safety of human life due to growing terrorism;

therefore, there is a need of developing low cost sensors with high detectability and selectivity. Nitroaromatic explosives can be detected using GO/nanomaterial sensors which have high surface area and large accumulation capacity with respect to analytes having  $\pi$  electron structure. It has been observed that the analytical signals are amplified. The functional groups present on the GO form strong hydrogen bonds with OH and  $\text{NO}_2$  groups of nitroaromatic compounds. The aromatic structure facilitates  $\pi$  stacking and the positive charge on the nitrogen atom generates electrostatic interactions which promote high loading of nitroaromatic analyte on GO (Li et al., 2012a, 2012b; Tang et al., 2010).

GO in conjugation with multiwalled carbon nanotubes (MWCNTs) is capable of detecting carcinogenic organic pollutant 1,3-dinitrobenzene which shows highly negative toxic impacts resulting in health problems. Due to large surface area of MWCNTs, they have been proved to be excellent electrode

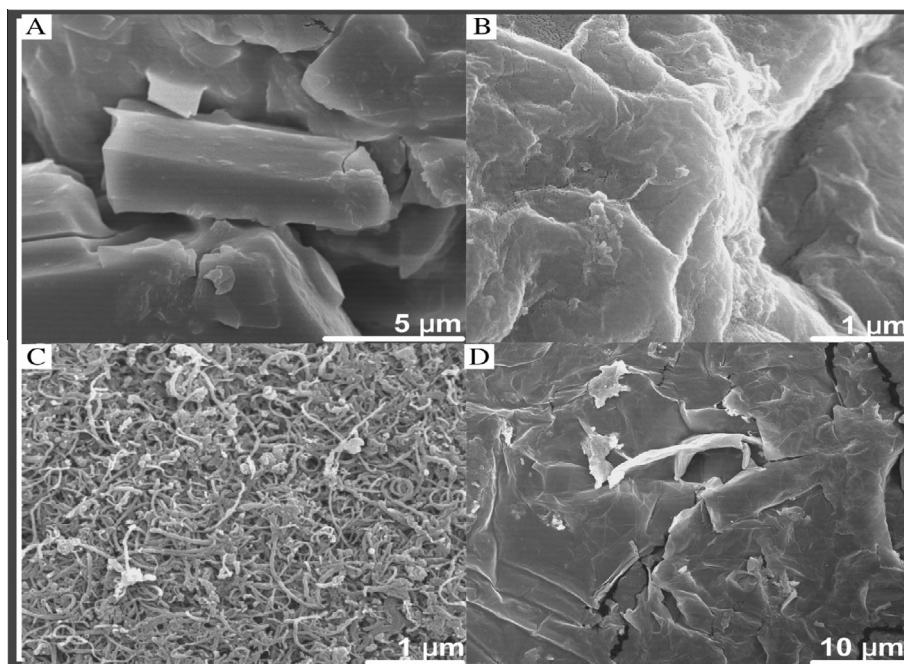


**Figure 20** (A)  $\beta$ -CD, (B) GO, (C) MWCNTs, (D)  $\beta$ -CD/MWCNTs/GO. Reproduced with permission Li et al. (2014a, 2014b).

**Table 1** Summary of GO based biosensors.

Sensor type	Analyte detected	Detection limit	Efficiency	Mechanism	Advantage	Citation
DNA	ssDNA	–	97%	Strong adsorption of ssDNA on GO	Sensitive & selective to target molecule	Lu et al. (2009a, 2009b, 2009c)
DNA nanoprobe	DNA	100 pM	~100%	$\pi$ -stacking interaction	Multicolor DNA analysis	He et al. (2010)
Molecular beacon (MB)	DNA	With 2 mL sample, 150 pM	–	Covalent interaction	Resistant to non-specific probe displacement	Huang and Liu (2012)
DNA	ssODN (oligodeoxyribonucleotide)	–	> 99%	$\pi$ - $\pi$ interaction	Broad range of DNA detection sensitivity & media dependence	Hong et al. (2012)
rGO-organic dye nanoswitch	Hg <sup>2+</sup>	2.8 nM	98.6%	$\pi$ - $\pi$ stacking interaction	Inexpensive, label-free, sensitive & selective detection of Hg <sup>2+</sup> without the interference of other metal ions	Huang et al. (2011)
Nanocomposite (rhodamine 6G (R6G) and GO)	DNA	0.01 nM	–	Strong ionic & $\pi$ - $\pi$ stacking interaction	Specific detection of analytes through simple ion-exchange process	Wang et al. (2012a, 2012b)
Glucose	Glucose	0.1 $\mu\text{mol L}^{-1}$	–	$\pi$ stacking interaction	Successfully determine glucose in human blood serum samples	Zhang et al. (2014)
COOH-GO	Glucose	$5 \times 10^{-8}$ to $1 \times 10^6 \text{ mol L}^{-1}$	–	$\pi$ - $\pi$ & hydrophobic interactions	Environmental monitoring & medical diagnostics	Song et al. (2010)
CoO <sub>x</sub> NPs/ERGO	Glucose	2 $\mu\text{M}$	–	–	Enzyme-free, reproducible, long-term performance stability	Li et al. (2014a, 2014b)
CuO/GO composite	Glucose	0.69 $\mu\text{M}$	–	Electron transfer reactions	Long term stability, good reproducibility, high selectivity, accurate measurement in real serum samples	Song et al. (2013)
Glucose	Glucose	6.5 $\mu\text{M}$	–	–	Non-toxicity, biocompatibility, biodegradability, promising matrix for enzyme immobilization	Peng et al. (2014)
Glucose	Glucose	40.8 $\mu\text{M}$	–	Electron tunneling pathway	Results similar to clinical analyzer	Shamsipur and Tabrizi (2014)
Glucose	Glucose	0.001 mM	–	–	High sensitivity and good stability, could be extended to the immobilization of other biomolecules	Hossain and Park (2014)
Tyrosine	L-tyrosine	4.4 nM	–	$\pi$ - $\pi$ stacking interaction	Enhanced electrocatalytic activity to the oxidation of L-tyrosine, direct determination in real samples without complicated and time consuming pretreatments	Li et al. (2013a, 2013b)

**Table 1** (continued)

Sensor type	Analyte detected	Detection limit	Efficiency	Mechanism	Advantage	Citation
Vitamin	Vitamin E	3.5 nM	–	$\pi$ - $\pi$ stacking interaction	Simple, rapid and accurate optosensing method	Liu et al. (2013a, 2013b)
MB	Biomolecules	12 nM	97.6%	$\pi$ - $\pi$ stacking interaction	High sensitivity, good selectivity, used for both quantification of nucleic acid & single nucleotide polymorphism, could be applied for detection of aptamer-specific molecules	Dong et al. (2010)
Protein	Protein	–	–	Direct $\pi$ stacking interaction	Robust operability in sensing platform, high precision in sensitivity	Kim et al. (2013a, 2013b)
Thrombin	Thrombin	3 pM–0.3 $\mu$ M	–	$\pi$ - $\pi$ stacking interaction	Fabrication involves solid state electrochemistry not involving the use of corrosive/toxic chemicals	Loo et al. (2013a, 2013b)
surface plasmon resonance (SPR)	Human IgG	4 times lower than that based on MPA (3-mercaptopropionic acid)	–	Specific antibody–antigen interaction	Successful immobilization	Zhang et al. (2013)
GO nanosheet based biosensor	ATP & GTP	–	–	$\pi$ - $\pi$ stacking interaction	Analyze multiple analytes in living cells	Wang et al. (2014)
Aptasensor	ATP	1 nM	–	$\pi$ - $\pi$ stacking interaction	Simple, cost-effective, probe does not require labeling, large fluorescence signals	Ning et al. (2014)
Fluorescent aptamer	<i>S. typhimurium</i>	100 CFU mL <sup>-1</sup>	–	$\pi$ - $\pi$ stacking interaction	Simple, sensitive, broad prospects in pathogen detection	Duan et al. (2014)
Aptamer modified QDs	Aflatoxin B1 (AFB1)	1.0 nM	–	$\pi$ - $\pi$ stacking interaction	Simple, fast, cost-effective, promising for analysis of mycotoxins	Lu et al. (2015)
Electrochemical	H <sub>2</sub> O <sub>2</sub>	0.01 $\mu$ M	–	–	Disposable, rapid, cost-effective, on field analysis of H <sub>2</sub> O <sub>2</sub> in food stuffs	Zhang et al. (2011a, 2011b)
Dz/nGO complex	Hepatitis C virus	–	95%	$\pi$ - $\pi$ stacking interaction	Potential theranostic nanomedicine for treating viral infection	Kim et al. (2013a, 2013b)
Drug	DCF (diclofenac)	0.09 $\mu$ M	–	–	Good reproducibility, repeatability, selectivity, promising application for clinical & pharmaceutical	Karuppiyah et al. (2015)
Electrochemical	4-Nitrophenol	0.02 $\mu$ M	–	$\pi$ - $\pi$ stacking interaction	Simple, sensitive & quantitative detection	Li et al. (2012a, 2012b)

(continued on next page)

**Table 1** (continued)

Sensor type	Analyte detected	Detection limit	Efficiency	Mechanism	Advantage	Citation
Electrochemical	1,3-Dinitrobenzene	5.0 nM	–	$\pi$ -donor–acceptor interactions	Long term stability, successfully employed in spiked soil & water samples, efficient assay in target detection	Li et al. (2014a, 2014b)
Remote WMS	<i>Escherichia coli</i>	60 cells/mL	–	–	Sensor response to any gram negative bacteria, rapid detection	Lu et al. (2009a, 2009b, 2009c)
WMS	Uranyl ( $\text{UO}_2^{2+}$ )	$2.87 \times 10^{-9}$ M	–	$\pi$ -stacking interactions	In-situ and real time assays for radioactive metal ions, wireless, low cost	Yin et al. (2013a, 2013b)
Acetylcholinesterase	Organophosphorus pesticides (OPs)	4.14 $\text{pg mL}^{-1}$ for malathion 1.15 $\text{pg mL}^{-1}$ for carbaryl	–	Strong hydrogen bonding interaction & reversible bonding	Short response time, good stability, high sensitivity, direct analysis of practical samples	Zhao et al. (2015a, 2015b)
Poly(3,4-ethylenedioxythiophene) PEDOT–GO	Nitrite	1.2 $\mu\text{M}$	–	$\pi$ – $\pi$ stacking interaction & electrostatic adsorption	Low cost, stable, high catalytic activity	Liu et al. (2011a, 2011b, 2011c)
Glucose	$\text{H}_2\text{O}_2$ & glucose	$4 \times 10^{-6}$ M	–	–	Simple, detection in human blood samples, promising applications in analytical & electroanalytical chemistry	Lu et al. (2011)
Au nanostructures/GO	4-Nitrophenol	–	–	$\pi$ – $\pi$ stacking interaction	Green, cost-effective, high catalytic activity	Zhang et al. (2011a, 2011b)
Immunosensor	Antibody–antigen (rabbit IgG–anti-rabbit IgG) interactions	0.67 nM	–	$\pi$ stacking interaction	Simple, portable, robust, suitable for developing electrochemical sensors	Roy et al. (2011)
Gas	$\text{NO}_2$	20 ppb	–	Hydrogen and covalent bonding	Simple, efficient, sensitive, environment friendly	Preziosa et al. (2013)

material for biosensing applications. The presence of hydrophilic groups in GO improves the film-forming property of modified electrodes. Li and coworkers fabricated glassy carbon electrode (GCE) modified with  $\beta$ -cyclodextrin ( $\beta$ -CD) MWCNTs and GO for the detection of 1,3-dinitrobenzene (Li et al., 2014a, 2014b). The electrochemical performance of the modified electrode was carried out by employing  $[\text{Fe}(\text{CN})_6]^{3-/4-}$  (1:1, molar ratio). It was observed that the voltammetric response of probe ions increased at MWCNTs/GCE surface and high redox peaks were obtained as compared to GO/GCE (Fig. 20). The excellent electronic properties of MWCNTs contribute to the increase in peak current densities. The redox response of the probe ions at MWCNTs/GO/GCE

was found to be in between GO/GCE and MWCNTs/GCE. This predicts the successful modification of MWCNTs/GO on GCE. As MWCNTs have high surface area,  $\beta$ -CD finds abundant binding sites on MWCNTs/GO surface. This leads to slow electron transfer between modifiers and electrode with low current response of modified electrode than that of MWCNTs/GO/GCE. This method offers a new way to detect explosives in trace amount and broadening the application of GO in the environmental analysis.

A recent development has been made in the construction of wireless magnetoelastic sensor (WMS) with high sensitivity, low cost, remote query and easy portability (Li et al., 2010a, 2010b; Lu et al., 2009a, 2009b, 2009c). This sensor is used

for the detection of uranyl ( $\text{UO}_2^{2+}$ ) since, uranium metal raises special concern because of its high toxicity and radioactivity (Li and Zhang, 2012). The important step in the designing of this sensor is to build a selective surface having recognition sites for a specific analyte such that analytical signals could be generated from the interaction between the analyte and the surface. For the recognition of  $\text{UO}_2^{2+}$ , DNAzyme was used and ssDNA was adsorbed on the GO surface. The substrate was cleaved by DNAzyme resulting into three ssDNA fragments in the presence of  $\text{UO}_2^{2+}$  and adsorbed onto the sensor by  $\pi$ -stacking interactions. The decrease of resonance frequency of sensor was in linear response to the concentration of uranyl ions. Also it was observed that the signal of the sensor could be enhanced in the presence of Au NPs. The sensor was found to have detection limit of  $2.87 \times 10^{-9}$  M and it avoided the interference of some metals such as  $\text{Cu}^{2+}$ ,  $\text{Fe}^{2+}$ ,  $\text{Fe}^{3+}$ ,  $\text{Hg}^{2+}$  and  $\text{Tb}^{3+}$  (Yin et al., 2013a, 2013b).

Organophosphorus pesticides (OPs) are extensively used in the agricultural field due to their high insecticidal activity. These pesticides are hazardous to human health as they are toxic to acetylcholinesterase (AChE) which is essential for the function of central nervous system. Therefore, it is essential to develop a biosensor which could detect trace levels of pesticides with high sensitivity. Biosensors based on acetylcholinesterase (AChE) have attracted attention because of their fast response and high sensitivity (Li et al., 2013a, 2013b). When AChE is immobilized on the electrode surface, it causes hydrolysis of acetylcholine chloride (ATCl) to an electro-active product thiocholine (TCh) which shows irreversible oxidation peak at about 0.68 V as the indication of presence of pesticide (Ivano et al., 2003). Zhao et al., synthesized ERGO-Au NPs- $\beta$ -CD deposited on GCE followed by the electrodeposition of Prussian blue (PB) nanoparticle-chitosan (CS) composite via one step direct electrodeposition approach. This process is very simple, fast and environmentally benign. The hydroxyl groups of  $\beta$ -cyclodextrin ( $\beta$ -CD) interact with graphene thereby preventing its agglomeration and also it interacts with acetylcholine to improve the sensitivity of biosensor for the detection of pesticides. The cycling stability of an electrode is enhanced by combining PB with CS. The composite of PB-CS can open many opportunities for the robust, simple and selective detection of organophosphorus pesticides (Zhao et al., 2015a, 2015b). The sensor showed wide linear ranges of  $7.98\text{--}2.00 \times 10^3$   $\text{pg mL}^{-1}$  and  $4.3\text{--}1.00 \times 10^3$   $\text{pg mL}^{-1}$  with low detection limits of  $4.14$   $\text{pg mL}^{-1}$  and  $1.15$   $\text{pg mL}^{-1}$  for malathion and carbaryl, respectively.

The analytical parameters and summary of the reported GO based sensors have been tabulated in Table 1.

## 6. Conclusions and future prospects

GO is one of the unique carbon materials exhibiting many potential applications in the field of science and technology owing to its diverse physical and chemical properties. The characteristics of GO enhance the electron mobility and stability at room temperature. Presently, electrochemical reduction method is employed for the synthesis of GO and still modifications are required in the preparation methods for producing high quality GO materials for effective biosensing applications. The functionalization of GO leads to the adsorption of different biomolecules and other molecules for biosensing

application. Due to the presence of negative groups on GO, molecules such as DNA, glucose, amino acids, vitamins and other analytes easily bind onto the surface through  $\pi$ - $\pi$  stacking, hydrophobic interaction and hydrogen bonding. Langmuir-Hinshelwood, Eley-Rideal and displacement mechanism predicted that DNA could be easily adsorbed either in solution or in gas phase on the GO surface. Moreover, one of the important features of GO to act as a weak acid cation in the presence of charged organic molecules enables dyes to couple with it forming a complex which quenches the fluorescence thus, paving a way for the designing of novel biosensors.

The monitoring of glucose is very important for maintaining the blood-sugar levels and for this "turn-on" fluorescence technique has been developed where GO-ssDNA interactions cause the selective determination of glucose. Nanomaterial such as SWCNTs, QDs and other NPs have been used along with GO to increase the electron mobility. The fluorescence of nanomaterials is quenched by GO and sensing capability enhances owing to promoted charge transfer reactions. Bimetallic NPs (Pt and Pd) act as efficient glucose biosensors as enzymes and other biomolecules can be easily immobilized on their surface.

The reproducibility and stability issues have been solved by the fabrication of enzyme free GO biosensors. The fluorescent intensity ratio which increases linearly with increase in the concentration of analyte could be used for the detection or sensing of different proteins. Energy transfer is found to be plausible mechanism for the fluorescence quenching. The limitation of the detection of ATP/GTP molecules for the visualization of living cells has been overcome by the use of GO nanosheets which have good cell membrane permeability and low toxicity. GO NPs also serve as excellent electroactive labels for the sensing of thrombin protein with greater selectivity. GO biosensors have been found to play a vital role in food safety also which in the upcoming future will be very beneficial to the food industry, one of the major in the world. The presence of pesticides is very harmful to the environment and can be detected in trace amounts with high sensitive, robust and cost-effective GO based sensor which leads to the new insight for environmentalists. Food borne pathogens causing diarrheal diseases could be rapidly detected via turn-on/off fluorescence with high specificity without cross reaction with other pathogens. GO biosensors fabricated through inexpensive processes and with fast response have not only been used for the detection of pathogenic bacteria and fungi but also deadly viruses which infected 70–90% of the world human population. GO surface mimics that of virus cell wall and stops the infection.

The analytes such as explosives, toxins and pesticides posing hazardous risks to the living environment can be detected in trace amounts using GO sensors. The functional groups present on the GO surface form strong hydrogen bonds with the groups present in the analytes thereby leading to their detection.

It is very critical to understand the mechanisms for the application of GO in the construction of biosensors so that they could be developed in bulk. Though biocompatibility studies have been reported but still there is a need to assess their toxicity so that they could be employed more potentially for bioimaging and drug delivery to curb some of the deadly diseases for which therapeutic tools have not been fully explored. GO biosensors have a lot of capability in paving a way in the medical field, thereby reaching a new altitude.

Moreover, GO can act as an alternate material to solve the challenges related to the environmental issues by exploiting its high sensitivity and selectivity properties for the detection of toxic molecules in trace amounts. The major prospect to be addressed in the future is the increasing demand of the engineering of biosensors based on GO that will allow to monitor and detect the analytes with high selectivity and sensitivity at low cost.

### Acknowledgments

Our grateful acknowledgment goes to the Durban University of Technology and National Research Foundation of South Africa for the financial support.

### References

- Akhavan, O., 2011. Photocatalytic reduction of graphene oxides hybridized ZnO nanoparticles in ethanol. *Carbon* 49 (1), 11–18.
- Brodie, B.C., 1859. On the atomic weight of graphite. *Philos. Trans. R. Soc. Lond.* 149, 249–259.
- Brody, H., 2011. Hepatitis C. *Nature* 474 (7350), S1–S48.
- Cambaz, Z.G., Yushin, G., Osswald, S., Mochalin, V., Gogotsi, Y., 2008. Noncatalytic synthesis of carbon nanotubes, graphene and graphite on SiC. *Carbon* 46 (6), 841–849.
- Chang, H., Chang, C., Tsai, Y., Liao, C., 2012. Electrochemically synthesized graphene/polypyrrole composite and their use in super capacitor. *Carbon* 50 (6), 2331–2336.
- Chen, L., Tang, Y., Wang, K., Liu, C., Luo, S., 2011. Direct electrodeposition of reduced graphene oxide on glassy carbon electrode and its electrochemical applications. *Electrochem. Commun.* 13 (2), 133–137.
- Cheng, M.L., Tsai, B.C., Yang, J., 2011. Silver nanoparticle-treated filter paper as a highly sensitive surface-enhanced Raman scattering (SERS) substrate for detection of tyrosine in aqueous solution. *Anal. Chim. Acta* 708 (1–2), 89–96.
- Cheng, N., Wang, H., Li, X., Yang, X., Zhu, L., 2012. Amperometric glucose biosensor based on integration of glucose oxidase with palladium nanoparticles/reduced graphene oxide nanocomposite. *Am. J. Anal. Chem.* 3 (4), 312–319.
- Choudhary, S., Marquez, M., Alencastro, F., Spors, F., Zhao, Y., Tiwari, V., 2011. Herpes simplex virus type-1 (HSV-1) entry into human mesenchymal stem cells is heavily dependent on heparan sulfate. *J. Biomed. Biotechnol.* 2011, 264350.
- Chua, C.K., Pumera, M., 2013. Reduction of graphene oxide with substituted borohydrides. *J. Mater. Chem. A* 1, 1892–1898.
- Chua, C.K., Pumera, M., 2014. Chemical reduction of graphene oxide: a synthetic chemistry viewpoint. *Chem. Soc. Rev.* 43 (1), 291–312.
- Chung, C., Kim, Y.K., Shin, D., Ryoo, S.R., Hong, B.H., Min, D.H., 2013. Biomedical applications of graphene and graphene oxide. *Acc. Chem. Res.* 46 (10), 2211–2224.
- Compton, O.C., Jain, B., Dikin, D.A., Abouimrane, A., Amine, K., Nguyen, S.T., 2011. Chemically active reduced graphene oxide with tunable C/O ratios. *ACS Nano* 5 (6), 4380–4391.
- Compton, O.C., Nguyen, S.T., 2010. Graphene oxide, highly reduced graphene oxide, and graphene: versatile building blocks for carbon-based materials. *Small* 6 (6), 711–723.
- Dikin, D.A., Stankovich, S., Zimney, E.J., Piner, R.D., Dommett, G.H.B., Evmenenko, G., Nguyen, S.T., Ruoff, R.S., 2007. Preparation and characterization of graphene oxide paper. *Nature* 448 (7152), 457–460.
- Ding, Y., Wang, Y., Su, L., Bellagamba, M., Zhang, H., Lei, Y., 2010. Electrospun Co<sub>3</sub>O<sub>4</sub> nanofibers for sensitive and selective glucose detection. *Biosens. Bioelectron.* 26 (6), 542–548.
- Dogan, H.O., Ekinici, D., Demir, U., 2013. Atomic scale imaging and spectroscopic characterization of electrochemically reduced graphene oxide. *Surf. Sci.* 611, 54–59.
- Dong, H., Gao, W., Yan, F., Ji, H., Ju, H., 2010. Fluorescence resonance energy transfer between quantum dots and graphene oxide for sensing biomolecules. *Anal. Chem.* 82 (13), 5511–5517.
- Dreyer, D.R., Todd, A.D., Bielawski, C.W., 2014. Harnessing the chemistry of graphene oxide. *Chem. Soc. Rev.* 43 (15), 5288–5301.
- Duan, Y.F., Ning, Y., Song, Y., Deng, L., 2014. Fluorescent aptasensor for the determination of *Salmonella typhimurium* based on graphene oxide platform. *Microchim. Acta* 181 (5–6), 647–653.
- Eigler, S., Dotzer, C., Hof, F., Bauer, W., Hirsch, A., 2013. Sulfur species in graphene oxide. *Eur. J. Chem.* 19 (29), 9490–9496.
- Forbeaux, I., Themin, J.M., Debever, J.M., 1998. Heteroepitaxial graphite on 6H-SiC (0001): interface formation through conduction-band electronic structure. *Phys. Rev. B* 58 (24), 16369–16373.
- Fu, Y., Zhang, J., Liu, H., Hiscox, W.C., Gu, Y., 2013. Ionic liquid-assisted exfoliation of graphite oxide for simultaneous and functionalization to with improved properties. *J. Mater. Chem. A* 1 (7), 2663–2674.
- Gao, X., Jang, J., Nagase, S., 2010. Hydrazine and thermal reduction of graphene oxide: reaction mechanisms, product structures, and reaction design. *J. Phys. Chem. C* 114, 832–842.
- Guo, H.L., Wang, X.F., Qian, Q.F., Wang, F.B., Xia, X.H., 2009. A green approach to the synthesis of graphene nanosheets. *ACS Nano* 3 (9), 2653–2659.
- He, H., Gao, C., 2010. Supraparamagnetic, conductive, and processable multifunctional graphene nanosheets coated with high density Fe<sub>3</sub>O<sub>4</sub> nanoparticle. *ACS Appl. Mater. Inter.* 2 (11), 3201–3210.
- He, S., Song, B., Li, D., Zhu, C., Qi, W., Wen, Y., Wang, L., Song, S., Fang, H., Fan, C., 2010. A graphene nanoprobe for rapid, sensitive and multicolor fluorescent DNA analysis. *Adv. Funct. Mater.* 20 (3), 453–459.
- Hernandez, Y., Nicolosi, V., Lotya, M., Blighe, F.M., Sun, Z., De, S., McGovern, I.T., Holland, B., Byrne, M., Gunko, Y.K., Boland, J.J., Niraj, P., Duesberg, G., Krishnamurthy, S., Goodhue, R., Hutchison, J., Scardaci, V., Ferrari, A.C., Coleman, J.N., 2008. High-yield production of graphene by liquid-phase exfoliation of graphite. *Nat. Nanotechnol.* 3, 563–568.
- Hilder, M., Winther-Jenson, B., Li, D., Forsyth, M., MacFarlane, D.R., 2011. Direct electro-deposition of graphene from aqueous suspensions. *Phys. Chem. Chem. Phys.* 13 (20), 9187–9193.
- Hong, B.J., An, Z., Compton, O.C., Nguyen, S.T., 2012. Tunable biomolecular interaction and fluorescence quenching ability of graphene oxide: application to “Turn-on” DNA sensing in biological media. *Small* 8 (16), 2469–2476.
- Hossain, M.F., Park, J.Y., 2014. Amperometric glucose biosensor based on Pt–Pd nanoparticles supported by reduced graphene oxide and integrated with glucose oxidase. *Electroanalysis* 26 (5), 940–951.
- Huang, P.J.J., Liu, J., 2012. Molecular beacon lighting up on graphene oxide. *Anal. Chem.* 84 (9), 4192–4198.
- Huang, W.T., Shi, Y., Xie, W.Y., Luo, H.Q., Li, N.B., 2011. A reversible fluorescence nanoswitch based on bifunctional reduced graphene oxide: use for detection of Hg<sup>2+</sup> and molecular logic gate operation. *Chem. Commun.* 47 (27), 7800–7802.
- Hummers Jr., W.S., Offemann, R.E., 1958. Preparation of graphitic oxide. *J. Am. Chem. Soc.* 80 (6), 1339.
- Inagaki, M., Kang, F., 2014. Graphene derivatives: graphane, fluorographene, graphene oxide, graphyne and graphdiyne. *J. Mater. Chem. A* 2 (33), 13193–13206.
- Ivano, A., Eotugyn, G., Budnikov, H., Ricci, F., Mosione, D., Paleschi, G., 2003. Cholinesterase sensors based on screen-printed electrodes for the detection of organophosphorous and carbamic pesticides. *Anal. Bioanal. Chem.* 377 (4), 624–631.
- Jiang, Y., Lu, Y., Li, F., Wu, T., Niu, L., Chen, W., 2012. Facile electrochemical codeposition of “clean” graphene-Pd

- nanocomposite as an anode catalyst for formic acid electrooxidation. *Electrochem. Commun.* 19, 21–24.
- Karupiah, C., Cheemalapati, S., Chen, S.M., Palanisamy, S., 2015. Carboxyl functionalized graphene oxide-modified electrode for the electrochemical determination of non-steroidal anti-inflammatory drug diclofenac. *Ionics* 21 (1), 231–238.
- Kashefi-Kheyrabadi, L., Mehrgardi, M.A., 2012. Aptamer-conjugated silver nanoparticles for electrochemical detection of adenosine triphosphate. *Biosens. Bioelectron.* 37 (1), 94–98.
- Khai, T.V., Na, H.G., Kwak, D.S., Kwon, Y.J., Ham, H., Shim, K.B., Kim, H.W., 2012. Significant enhancement of blue emission and electrical conductivity of N-doped graphene. *J. Mater. Chem.* 22 (34), 17992–18003.
- Kim, J., Cote, L.J., Kim, F., Huang, J., 2010. Visualization graphene based sheets by fluorescence quenching microscopy. *J. Am. Chem. Soc.* 132 (1), 260–267.
- Kim, S.K., Um, Y.M., Jang, J.R., Choe, W.S., Yoo, P.J., 2013a. Highly sensitive reduced graphene oxide impedance sensor harnessing  $\pi$ -stacking interaction mediated direct deposition of protein probes. *ACS Appl. Mater. Inter.* 5 (9), 3591–3598.
- Kim, S., Ryoo, S.R., Na, H.K., Kim, Y.K., Choi, B.H., Lee, Y., Kim, D.E., Min, D.H., 2013b. Deoxyribosome-loaded nano-graphene oxide for simultaneous sensing and silencing of the hepatitis C virus gene in liver cells. *Chem. Commun.* 49 (74), 8241–8243.
- Kim, K.S., Zhao, Y., Jang, H., Lee, S.Y., Kim, J.M., Ahn, J.H., Kim, P., Choi, J.Y., Hong, B.H., 2009. Large-scale pattern growth of graphene films for stretchable transparent electrodes. *Nature* 457 (7239), 706–710.
- Krishnan, D., Kim, F., Luo, J., Cruz-Silva, R., Cote, L.J., Jang, H.D., Huang, J., 2012. Energetic graphene oxide: challenges and opportunities. *Nano Today* 7 (2), 137–152.
- Laviron, E., 1974. Adsorption, autoinhibition and autocatalysis in polarography and in linear potential sweep voltammetry. *J. Electroanal. Chem.* 52 (3), 355–393.
- Lerf, A., He, H., Forster, M., Klinowski, J., 1998. Structure of graphite oxide revisited. *J. Phys. Chem. B* 102 (23), 4477–4482.
- Li, F., Feng, Y., Zho, C., Li, P., Tang, B., 2012a. A sensitive graphene oxide-DNA based sensing platform for fluorescence “turn-on” detection of bleomycin. *Chem. Commun.* 48 (1), 127–129.
- Li, H., Li, Y., Cheng, J., 2010a. Molecularly imprinted silica nanospheres embedded CdSe quantum dots for highly selective and sensitive optosensing of pyrethroids. *Chem. Mater.* 22 (8), 2451–2457.
- Li, J., Feng, H., Feng, Y., Liu, J., Liu, Y., Jiang, J., Qian, D., 2014a. A glassy electrode modified with  $\beta$ -cyclodextrin, multiwalled carbon nanotubes and graphene oxide for sensitive determination of 1,3-dinitrobenzene. *Microchim. Acta* 181 (11–12), 1369–1377.
- Li, J., Kuang, D., Feng, Y., Zhang, F., Xu, Z., Liu, M., 2012b. A graphene oxide-based electrochemical sensor for sensitive determination of 4-nitrophenol. *J. Hazard. Mater.* 201–202, 250–259.
- Li, J., Zhang, Y., 2012. Remediation technology for the uranium contaminated environment: a review. *Proc. Environ. Sci.* 13, 1609–1615.
- Li, S.J., Du, J.M., Chen, J., Mao, N.N., Zhang, M.J., Pang, H., 2014b. Electrodeposition of cobalt oxide nanoparticles on reduced graphene oxide: a two dimensional hybrid for enzyme-free glucose sensing. *J. Solid State Electrochem.* 18 (4), 1049–1056.
- Li, S., Li, Y., Chen, H., Horokawa, S., Shen, W., Simonian, A., Chin, B.A., 2010b. Direct detection of *Salmonella typhimurium* on fresh produce using phage based magnetoelastic biosensors. *Biosens. Bioelectron.* 26 (4), 1313–1319.
- Li, X., Cai, W., An, J., Kim, S., Nah, J., Yang, D., Piner, R., Velamakanni, A., Jung, I., Tutuc, E., Banerjee, S.K., Colombo, L., Ruoff, R.S., 2009. Large-area synthesis of high quality and uniform graphene films on copper foils. *Science* 324 (5932), 1312–1314.
- Li, Y., Bai, Y., Li, M., 2013a. Porous-reduced graphene oxide for fabricating an amperometric acetylcholinesterase biosensor. *Sens. Actuat.* 185, 706–712.
- Li, J., Kuang, D., Feng, Y., Zhang, F., Xu, Z., Liu, M., Wang, D., 2013b. Electrochemical tyrosine sensor based on glassy carbon electrode modified with a nanohybrid made from graphene oxide and multiwalled carbon nanotubes. *Microchim. Acta* 180 (1–2), 49–58.
- Liashkovich, L., Hafezib, W., Kumb, J.M., Oberleithner, H., Shahina, V.J., 2011. Nuclear delivery mechanism of herpes simplex virus type 1 genome. *Mol. Recogn.* 24 (3), 414–421.
- Liu, B., Sun, Z., Zhang, X., Liu, J., 2013a. Mechanisms of DNA sensing on graphene oxide. *Anal. Chem.* 85 (16), 7987–7993.
- Liu, C., Wang, K., Luo, S., Tang, Y., Chen, L., 2011a. Direct electrodeposition of graphene enabling the one-step synthesis of graphene-metal nanocomposite films. *Small* 7 (9), 1203–1206.
- Liu, H., Fang, G., Zhu, H., Li, C., Liu, C., Wang, S., 2013b. A novel ionic liquid stabilized molecularly imprinted optosensing material based on quantum dots and graphene oxide for specific recognition of vitamin E. *Biosens. Bioelectron.* 47, 127–132.
- Liu, M., Zhang, Q.A., Zho, H.M., Chen, S., Yu, H.T., Zhang, Y.B., Quan, X., 2011b. Controllable oxidation DNA cleavage-dependent regulation of graphene/DNA interaction. *Chem. Commun.* 47 (14), 4084–4086.
- Liu, N., Luo, F., Wu, H., Liu, Y., Zhang, C., Chen, J., 2008. One-step ionic-liquid-assisted electrochemical synthesis of ionic-liquid-functionalized graphene sheets directly from graphite. *Adv. Funct. Mater.* 18, 1518–1525.
- Liu, S., Tian, J., Wang, L., Luo, Y., Sun, X., 2011c. Production of stable aqueous dispersion of poly(3,4-ethylenedioxythiophene) nanorods using graphene oxide as a stabilizing agent and their application for nitrite detection. *Analyst* 136 (23), 4898–4902.
- Liu, Z., Liu, B., Ding, J., 2014. Fluorescent sensor using DNA-functionalized graphene oxide. *Anal. Bioanal. Chem.* 406 (27), 6885–6902.
- Loh, K.P., Bao, Q., Eda, G., Chhowalla, M., 2010. Graphene oxide as a chemically tunable platform for optical applications. *Nat. Chem.* 2 (12), 1015–1024.
- Loo, A., Bonanni, A., Pumera, M., 2013a. Thrombin aptasensing with inherently electroactive graphene oxide nanoplatelets as labels. *Nanoscale* 5 (11), 4758–4762.
- Loo, A., Bonanni, A., Pumera, M., 2013b. Inherently electroactive graphene oxide nanoplatelets as labels for specific protein-target recognition. *Nanoscale* 5 (17), 7844–7848.
- Lu, C.H., Yang, H.H., Zhu, C.L., Chen, X., Chen, G.N., 2009a. A graphene platform for sensing biomolecules. *Angew. Chem. Int. Ed.* 48 (26), 4785–4787.
- Lu, C.H., Zhu, C.L., Li, J., Liu, J.J., Chen, X., Yang, H.H., 2010. Using graphene to protect DNA from cleavage during cellular delivery. *Chem. Commun.* 46 (18), 3116–3118.
- Lu, J., Yang, J.X., Wang, J.Z., Lim, A., Wang, S., Poh, K.P., 2009b. One-pot synthesis of fluorescent carbon nanoribbons, nanoparticles, and graphene by the exfoliation of graphite in ionic liquids. *ACS Nano* 3, 2367–2375.
- Lu, Q., Lin, H., Ge, S., Luo, S., Cai, Q., Grimes, C.A., 2009c. Wireless remote-query, and high sensitivity of *Escherichia coli* 0157:H7 biosensor based on the recognition action of concanavalin A. *Anal. Chem.* 81 (14), 5846–5850.
- Lu, W., Luo, Y., Chang, G., Sun, X., 2011. Synthesis of functional SiO<sub>2</sub>-coated graphene oxide nanosheets decorated with Ag nanoparticles for H<sub>2</sub>O<sub>2</sub> and glucose detection. *Biosens. Bioelectron.* 26 (12), 4791–4797.
- Lu, Z., Chen, X., Wang, Y., Zheng, X., Li, C.M., 2015. Aptamer based fluorescence recovery assay for aflatoxin B1 using a quencher system composed of quantum dots and graphene oxide. *Microchim. Acta* 182 (3–4), 571–578.
- Ma, Q., Yu, W., Huang, H., Su, X., 2011. Determination of L-tyrosine based on luminescence quenching of Mn-doped ZnSe quantum dots in enzyme catalysis system. *J. Fluoresc.* 21 (1), 125–131.

- Makarov, V.L., Hirose, Y., Langmore, J.P., 1997. Long G tails at both ends of human chromosomes suggest a C strand degradation mechanism for telomere shortening. *Cell* 88 (5), 657–666.
- Manohar, S., Mantz, A.R., Bancroft, K.E., Hui, C.Y., Jagota, A., Vezenov, D.V., 2008. Peeling single stranded DNA from graphite surface to determine oligonucleotide binding energy by force spectroscopy. *Nano Lett.* 8 (12), 4365–4372.
- Marcano, D.C., Kosynkin, D.V., Berlin, J.M., Sinitskii, A., Sun, Z., Slesarev, A., Alemany, L.B., Lu, W., Tour, J.M., 2010. Improved synthesis of graphene oxide. *ACS Nano* 4 (8), 4806–4814.
- Mergeny, J.L., Lacroix, L., Teulade-Fichou, M.P., Hounsou, C., Guittat, L., Hoarau, M., Arimondo, P.B., Vigneron, J.P., Lehn, J.M., Riou, J.F., Garestier, T., Helene, C., 2001. Telomerase inhibitors based on quadruplex ligands selected by a fluorescence assay. *Proc. Natl. Acad. Sci. U.S.A.* 98, 3062–3067.
- Millour, S., Noel, L., Kadar, A., Chekri, R., Vastel, C., Sirot, B., Leblanc, J., Guerin, T., 2011. Pb, Hg, Cd, As, Sb and Al levels in foodstuffs from the 2nd French total diet study. *Food Chem.* 126 (4), 1787–1799.
- Morales-Narváez, E., Merkoçi, A., 2012. Graphene oxide as an optical biosensing platform. *Adv. Mater.* 24 (25), 3298–3308.
- Nel, A.E., Mädler, L., Velegol, D., Xia, T., Hoek, E.M.V., Somasundaran, P., Klaessig, F., Castronova, V., Thompson, M., 2009. Understanding biophysicochemical interactions at the nanobio interface. *Nat. Mater.* 8, 543–557.
- Ning, Y., Duan, Y., Feng, Y., Deng, L., 2014. Label-free fluorescent aptasensor based on graphene oxide self-assembled probe for the determination of adenosine triphosphate. *Anal. Lett.* 47 (14), 2350–2360.
- Novoselov, K.S., 2011. Graphene: materials in flatland (Nobel lecture). *Angew. Chem. Int. Ed.* 50 (31), 6986–7002.
- Novoselov, K.S., Geim, A.K., Morozov, S.V., Jiang, D., Zhang, Y., Dubonos, S.V., Grigorieva, L.V., Firsov, A.A., 2004. Electric field effect in atomically thin carbon films. *Science* 306 (5696), 666–669.
- Novoselov, K.S., Jiang, D., Schedin, F., Booth, T.J., Khotkevich, V.V., Morozov, S.V., Geim, A.K., 2005. Two-dimensional atomic crystals. *Proc. Natl. Acad. Sci. U.S.A.* 102, 10451–10453.
- Nurunnabi, Md., Parvez, K., Nafujjaman, Md., Revuri, V., Khan, H.A., Feng, X., Lee, Y.K., 2015. Bio-application of graphene oxide derivatives: drug/gene delivery, imaging, polymeric modification, toxicology, therapeutics and challenges. *RSC Adv.* 5 (52), 42141–42161.
- Park, J.S., Na, H.K., Min, D.H., Kim, D.E., 2013. Desorption of single-stranded nucleic acids from graphene oxide by disruption of hydrogen bonding. *Analyst* 138 (6), 1745–1749.
- Park, S., Ruoff, R.S., 2009. Chemical methods for the production of graphene. *Nat. Nanotechnol.* 4, 217–224.
- Paredes, J.I., Villar-Rodil, S., Fernandez-Merino, M.J., Guardia, L., Martinez-Alonso, A., Tascon, J.M.D., 2011. Environmentally friendly approaches toward the mass production of process able graphene from graphite oxide. *J. Mater. Chem.* 21, 298–306.
- Pariasamy, M., Thirumalaikumar, M., 2000. Methods of enhancement of reactivity and selectivity of sodium borohydride for application in organic synthesis. *J. Organomet. Chem.* 609, 137–151.
- Peng, H., Huang, Z., Zheng, Y., Chen, W., Liu, A., Lin, X., 2014. A novel nanocomposite matrix based on graphene oxide and ferrocene-branched organically modified sol-gel/chitosan for biosensor application. *J. Solid State Electrochem.* 18 (7), 1941–1949.
- Peng, X., Liu, X., Diamond, D., Lau, K.T., 2011. Synthesis of electrochemically-reduced graphene oxide film with controllable size and thickness and its use in super capacitor. *Carbon* 49 (11), 3488–3496.
- Ping, J., Wang, Y., Fai, K., Wu, J., Ying, Y., 2011. Direct electrochemical reduction of graphene oxide on ionic liquid doped screen printed electrode and its electrochemical biosensing applications. *Biosens. Bioelectron.* 28, 204–209.
- Plym Forshell, L., Wierup, M., 2006. *Salmonella* contamination: a significant challenge to the global marketing of animal food products. *Rev. Sci. Tec.* 25 (2), 541–554.
- Preziosa, S., Perrozzì, F., Giancaterini, L., Cantalini, C., Treossi, E., Palermo, V., Nardone, M., Santucci, S., Ottaviano, L., 2013. Graphene oxide as a practical solution to high sensitivity gas sensing. *J. Phys. Chem. C* 117 (20), 10683–10690.
- Pumera, M., 2011. Graphene in biosensing. *Mater. Today* 14 (7–8), 308–315.
- Qi, B., He, L., Bo, X., Yang, H., Guo, L., 2011. Electrochemical preparation of free-standing few-layer graphene through oxidation-reduction cycling. *Chem. Eng. J.* 171 (1), 340–344.
- Razmi, H., Nasiri, H., Mohammad-Rezaei, R., 2011. Amperometric determination of L-tyrosine by an enzymeless sensor based on a carbon ceramic electrode modified with copper oxide nanoparticles. *Microchim. Acta* 173, 59–64.
- Richard, E., Heutte, N., Sage, L., Pottier, D., Bouchart, V., Lebailly, P., Garon, D., 2007. Toxicogenic fungi and mycotoxins in mature corn silage. *Food Bioprocess Tech.* 45 (12), 2420–2425.
- Roy, S., Soin, N., Bajpai, R., Misra, D.S., McLaughlin, James A., Roy, S.S., 2011. Graphene oxide for electrochemical sensing applications. *J. Mater. Chem.* 21 (38), 14725–14731.
- Sametband, M., Kalt, I., Gedanken, A., Sarid, R., 2014. Herpes simplex virus type-1 attachment inhibition by functionalized graphene oxide. *ACS Appl. Mater. Inter.* 6 (2), 1228–1235.
- Sánchez-Machado, D.I., Chavira-Willgs, B., López-Cervantes, J., 2008. High-performance liquid chromatography with fluorescence detection for quantification of tryptophan and tyrosine in a shrimp waste protein concentrate. *J. Chromatogr. B* 863 (1), 88–93.
- Schenze, J., Forrer, H.R., Vogelgsang Hungerbühler, K., Bucheli, T.D., 2012. Mycotoxins in the Environment: I. Production and emission from an agricultural test field. *Environ. Sci. Technol.* 46 (24), 13067–13075.
- Shamsipur, M., Tabrizi, M.A., 2014. Achieving direct electrochemistry of glucose oxidase by one step electrochemical reduction of graphene oxide and its use in glucose sensing. *Mater. Sci. Eng. C* 45, 103–108.
- Shao, W., Liu, H., Liu, X., Wang, S., Zhang, R., 2015. Anti-bacterial performances and biocompatibility of bacterial cellulose/graphene oxide composites. *RSC Adv.* 5 (7), 4795–4803.
- Sharma, P.S., D'Souza, F., Kutner, W., 2013. Graphene and graphene oxide materials for chemo- and biosensing of chemical and biochemical hazards. *Top. Curr. Chem.* 348, 237–265.
- Shen, J., Shi, M., Li, N., Yan, B., Ma, H., Hu, Y., Ye, M., 2010. Facile synthesis and application of Ag-chemically converted graphene nanocomposite. *Nano Res.* 3 (5), 339–349.
- Shin, H.J., Kim, K.K., Benayad, A., Yoon, S.M., Park, H.K., Jung, I., Jin, M.H., Jeong, H., Kim, J.M., Choi, J., Lee, Y.H., 2009. Efficient reduction of graphite oxide by sodium borohydride and its effect on electrical conductance. *Adv. Funct. Mater.* 19 (12), 1987–1992.
- Singh, V., Joung, D., Zhai, L., Das, S., Khondaker, S.I., Seal, S., 2011. Graphene based materials: past, present and future. *Prog. Mater. Sci.* 56 (8), 1178–1271.
- Song, J., Xu, L., Zhou, C., Xing, R., Dai, L., Song, H., 2013. Synthesis of graphene oxide based CuO nanoparticles composite electrode for highly enhanced non-enzymatic glucose detection. *ACS Appl. Mater. Inter.* 5 (24), 12928–12934.
- Song, Y., Qu, K., Zho, C., Ren, J., Qu, X., 2010. Graphene oxide: intrinsic peroxidase catalytic activity and its application to glucose detection. *Adv. Mater.* 22 (19), 2206–2210.
- Stankovich, S., Dikin, D.A., Dommett, G.H.B., Kohkass, K.M., Zimney, E.J., Stach, E.A., Piner, R.D., Nguyen, S.T., Ruoff, R.S., 2006a. Graphene-based composite materials. *Nature* 442 (7100), 282–286.
- Stankovich, S., Piner, R.D., Chen, X.Q., Wu, N.Q., Nguyen, S.T., Ruoff, R.S., 2006b. Stable aqueous dispersion of graphitic nanoplatelets via the reduction of exfoliated graphite oxide in the

- presence of poly(sodium 4-styrenesulfonate). *J. Mater. Chem.* 16, 155–158.
- Staudenmaier, L., 1898. Verfahren zur Darstellung der Graphitsäure. *Ber. Dtsch. Chem. Ges.* 31 (2), 1481–1487.
- Subramanian, R.P., Geratgty, R.J., 2007. Herpes simplex virus type 1 mediates fusion through a hemifusion intermediate by sequential activity of glycoproteins D, H, L, and B. *Proc. Natl. Acad. Sci. U.S.A.* 104 (8), 2903–2908.
- Swathi, R.S., Sebastian, K.L., 2008. Resonance energy transfer from a dye molecule to graphene. *J. Chem. Phys.* 129 (5), 054703.
- Swathi, R.S., Sebastian, K.L., 2009. Long range resonance energy transfer from a dye molecule to graphene has (distance)<sup>(-4)</sup> dependence. *J. Chem. Phys.* 130 (8), 086101.
- Szabo, T., Berkesi, O., Dekany, I., 2005. DRIFT study of deuterium-exchanged graphite oxide. *Carbon* 43 (15), 3186–3189.
- Talyzin, A.V., Sundqvist, B., Szabó, T.S., Dékány, I., Dmitriev, V., 2009. Pressure-induced insertion of liquid alcohols into graphite oxide structure. *J. Am. Chem. Soc.* 131 (51), 18445–18449.
- Talyzin, A.V., Solozhenko, V.L., Kurakevych, O.O., Szabó, T.S., Dékány, I., Kurnosov, A., Dmitriev, V., 2008. Colossal pressure-induced lattice expansion of graphite oxide in the presence of water. *Angew. Chem. Int. Ed.* 47 (43), 8268–8271.
- Tang, L., Feng, H., Cheng, J., Li, J., 2010. Uniform and rich-wrinkled electrophoretic deposited graphene film: a robust electrochemical platform for TNT sensing. *Chem Commun.* 46 (32), 5882–5884.
- Tang, L., Li, X., Ji, R., Teng, K.S., Tai, G., Ye, J., Wei, C., Lau, S.P., 2012. Bottom-up synthesis of large-scale graphene oxide nanosheets. *J. Mater. Chem.* 22 (12), 5676–5683.
- Vinu Mohan, A.M., Aswini, K.K., Starvin, A.M., Biju, V.M., 2013. Amperometric detection of glucose using Prussian blue-graphene oxide modified platinum electrode. *Anal. Meth.* 5 (7), 1764–1770.
- Walcarius, A., Minter, S.D., Wang, J., Lin, Y., Merkoçi, A., 2013. Nanomaterials for bio-functionalised electrodes: recent trends. *J. Mater. Chem. B* 1 (38), 4878–4908.
- Wang, G., Wang, B., Park, J., Yang, J., Shen, X., Yao, J., 2009a. Synthesis of enhanced hydrophilic and hydrophobic graphene oxide nanosheets by a solvothermal method. *Carbon* 47 (1), 68–72.
- Wang, G.X., Yang, J., Park, J., Guo, X.L., Wang, B., Liu, H., Yao, J., 2008a. Facile synthesis and characterization of graphene nano sheets. *J. Phys. Chem. C* 112 (22), 8192–8195.
- Wang, H., Chen, T., Wu, S., Chu, X., Yu, R., 2012a. A novel biosensor strategy for screening G-quadruplex ligand based on graphene oxide sheets. *Biosens. Bioelectron.* 34 (1), 88–93.
- Wang, J., Manga, K.K., Bao, Q., Loh, K.P., 2011a. High-yield synthesis of few-layer graphene flakes through electrochemical expansion of graphite in propylene carbonate electrolyte. *J. Am. Chem. Soc.* 133 (23), 8888–8891.
- Wang, W., Lee, G.J., Jang, K.J., Cho, T.S., Kim, S.K., 2008b. Real-time detection of Fe. EDTA/H<sub>2</sub>O<sub>2</sub>-induced DNA cleavage by linear dichroism. *Nucleic Acids Res.* 36 (14), e85.
- Wang, X., Zhong, S., He, Y., Song, G., 2012b. A graphene oxide-rhodamine 6G nanocomposite as turn-on fluorescence probe for selective detection of DNA. *Anal. Meth.* 4 (2), 360–362.
- Wang, Y., Liu, J., Liu, L., Sun, D.D., 2011b. High-quality reduced graphene oxide-nanocrystalline platinum hybrid materials prepared by simultaneous co-reduction of graphene oxide and chloroplatinic acid. *Nano Res. Lett.* 6, 241–248.
- Wang, Y., Tang, L., Li, Z., Lin, Y., Li, J., 2014. In-situ simultaneous monitoring of ATP and GTP using a graphene oxide nanosheet-based sensing platform in living cells. *Nat. Protoc.* 9 (8), 1944–1955.
- Wang, Z., Zhou, X., Zhang, J., Boef, F., Zhang, H., 2009b. Direct electrochemical reduction of single-layer graphene oxide and subsequent functionalization with glucose oxidase. *J. Phys. Chem. C* 113 (32), 14071–14075.
- Williams, O., Seger, B., Kamat, P., 2008. TiO<sub>2</sub>-graphene nanocomposites. UV-assisted photocatalytic reduction of graphene oxide. *ACS Nano* 2 (7), 1487–1491.
- Wu, J., Wang, Y.S., Yang, X.Y., Liu, Y.Y., Yang, J.R., Yang, R., Zhang, N., 2012. Graphene oxide used as a carrier for adriamycin can reverse drug resistance in breast cancer cells. *Nanotechnology* 23 (35), 355101.
- Xia, Z.Y., Pezzini, S., Treossi, E., Giambastiani, G., Corticelli, F., Morandi, V., Zanelli, A., Bellani, V., Palermo, V., 2013. The exfoliation of graphene in liquids by electrochemical, chemical, and sonication-assisted techniques: a nanoscale study. *Adv. Funct. Mater.* 23 (37), 4684–4693.
- Xiang, C., Li, M., Zhi, M., Manivannan, A., Wu, N., 2013. A reduced graphene oxide/Co<sub>3</sub>O<sub>4</sub> composite for super capacitor electrode. *J. Power Sources* 226, 65–70.
- Yang, K., Gong, H., Shi, X., Wan, J., Zhang, Y., Liu, Z., 2013a. In vivo biodistribution and toxicology of functionalized nano-graphene oxide in mice after oral and intraperitoneal administration. *Biomaterials* 34 (11), 2787.
- Yang, Y., Zhuo, J.W., Zhang, Y.S., Zhou, Q., Zhang, X.H., Chen, J.H., 2013b. Sensitive electrochemical detection of hydroxyl radical based on MBs-DNA-AgNPs nanocomposite. *Sens. Actuat. B: Chem.* 182, 504–509.
- Yin, D., Li, Y., Lin, H., Guo, B., Du, Y., Li, X., Jia, H., Zho, X., Tang, J., Zhang, L., 2013a. Functional graphene oxide as a plasmid-based stat3 siRNA carrier inhibits mouse malignant melanoma growth in vivo. *Nanotechnology* 24 (10), 105102.
- Yin, J.C., Wang, Y.S., Zhou, B., Xiao, X.L., Xue, J.H., Wang, J.C., Wang, Y.S., Qian, Q.M., 2013b. A wireless magnetoelastic sensor for uranyl using DNAzyme-graphene oxide and gold nanoparticles based amplification. *Sens. Actuat.* 188, 147–155.
- Zhang, B., Cui, Y., Chen, H., Liu, B., Guonam, C., Tang, D., 2011a. A new electrochemical biosensor for determination of hydrogen peroxide in food based on well-dispersive gold nanoparticles on graphene oxide. *Electroanalysis* 23 (8), 1821–1829.
- Zhang, H., Huang, H., Liu, Z., Su, X., 2014. A turn-on fluorescence-sensing technique for glucose determination based on graphene oxide-DNA interaction. *Anal. Bioanal. Chem.* 406 (27), 6925–6932.
- Zhang, H., Sun, Y., Gao, S., Zhang, J., Zhang, H., Song, D., 2013. A novel graphene oxide-based surface plasmon resonance biosensor. *Small* 15 (9), 2537–2540.
- Zhang, Y., Liu, S., Lu, W., Wang, L., Tian, J., Sun, X., 2011b. *In-situ* green synthesis of Au nanostructures on graphene oxide and their applications for catalytic reduction of 4-nitrophenol. *Catal. Sci. Technol.* 1 (7), 1142–1144.
- Zhao, H., Ji, X., Wang, B., Wang, N., Li, X., Ni, R., Ren, J., 2015a. An ultra-sensitive acetylcholinesterase biosensor based on reduced graphene oxide-Au nanoparticles-β-cyclodextrin/Prussian blue-chitosan nanocomposites for organophosphorus pesticide detection. *Biosens. Bioelectron.* 65, 23–30.
- Zhao, J., Liu, L., Fen, L., 2015b. Graphene Oxide: Physics and Applications. Springer Briefs in Physics, [http://dx.doi.org/10.1007/978-3-662-44829-8\\_3](http://dx.doi.org/10.1007/978-3-662-44829-8_3).
- Zhu, X., Xu, S., 2010. Determination of L-tyrosine by β-cyclodextrin sensitized fluorescence quenching method. *Spectrochim. Acta A* 77 (3), 566–571.
- Zhu, Y., Kai, W., Piner, R.D., Velamakanni, A., Ruoff, R.S., 2009. Transparent self-assembled films of reduced graphene oxide platelets. *Appl. Phys. Lett.* 95, 103104–103108.
- Zhu, Y., Murali, S., Cai, W., Li, X., Suk, J.W., Potts, J.R., Ruoff, R.S., 2010. Graphene and graphene oxide: synthesis, properties, and applications. *Adv. Mater.* 22 (46), 3906–3924.
- Zubir, N.A., Yacou, C., Motuzas, J., Zhang, X., Diniz da Costa, J.C., 2014. Structural and functional investigation of graphene oxide-Fe<sub>3</sub>O<sub>4</sub> nanocomposites for the heterogeneous Fenton-like reaction. *Sci. Rep.* 4, 4583–4594.